RSC Advances

REVIEW

View Article Online
View Journal | View Issue

Cite this: *RSC Adv.*, 2024, **14**, 20714

Recent progress on CO_2 separation membranes†

Yuheng Fan, [a] Weichu Yu, *[ab] Aibin Wu, [a] Wenming Shu [a] and Ying Zhang[a]

Received 17th January 2024
Accepted 15th June 2024

DOI: 10.1039/d4ra00444b

rsc.li/rsc-advances

Presently, excessive carbon dioxide emissions represent a critical environmental challenge. Thus, urgent efforts are required to develop environmentally friendly and low-energy technologies for carbon dioxide treatment. In this case, membrane separation technology stands out as a promising avenue for CO_2 separation, with selective membrane materials of high permeability playing a pivotal role in this process. Herein, we categorize CO_2 separation membranes into three groups: inorganic membranes, organic membranes, and emerging membranes. Moreover, representative high-performance membranes are introduced and their synthesis methods, gas separation performances, and applications are examined. Furthermore, a brief analysis of the challenges encountered by carbon dioxide separation membrane materials is provided together with a discussion on the future research direction. It is expected that this review will provide some potential insights and guidance for the future development of CO_2 separation membranes, which can promote their development.

1. Introduction

CO_2 capture, utilization, and storage (CCUS) technology stands out as the most effective approach to mitigate greenhouse gas emissions, attracting considerable attention worldwide.[1,2] CCUS technology is based on the capture and separation of carbon dioxide.[3] To realize the objective of capturing and isolating carbon dioxide, membrane separation has emerged as the prevalent method. This technique allows for the selective permeation of carbon dioxide through physical or chemical interactions between carbon dioxide and the membrane.

Research on carbon dioxide membrane separation methods centered around the preparation and acquisition of high-efficiency membranes. Currently, extensively studied CO_2 separation membranes include inorganic, organic, and emerging membranes. Inorganic membranes primarily consist of silica, zeolite, and graphene membranes. Organic membranes include cellulose, polyamide, polysulfone, and polyether membranes. Emerging membranes include composite, metal–organic framework (MOF), zeolitic imidazolate framework (ZIF), carbon molecular sieve (CMS), polymers of intrinsic microporosity (PIM), and facilitated transport membranes. With its notable advantages of low energy consumption and high separation efficiency, the membrane separation method is rapidly emerging as globally advancing technology for carbon dioxide capture and separation.[4]

In the case of concentration difference or pressure difference on both sides of a gas film, the mixed gas to be selectively separated passes through the gas separation film, and gas separation is realized on the basis of the difference in the rate of different components in the mixed gas passing through the gas film. The selectivity of gas separation membranes represents the degree of separation of the required gas molecules from other molecules, and the separation factor represents the efficiency of gas separation.[5] The amount of gas passing through a membrane with a certain area and thickness per unit time and differential pressure can be determined. Robeson upper limit represents the limit of the separation performance of homopolymer membranes for a specific gas pair (CO_2/CH_4, CO_2/N_2, *etc.*) and is useful for guiding breakthroughs in optimizing the structure/performance of polymer membranes. The upper limit reflects the trade-off effect, whereby an increase in permeability leads to a decrease in selectivity and *vice versa*. Fitting parameters for Robeson upper bounds (2008) and proposed CO_2/N_2 upper bounds are determined using the formula $P_x = 30.967 \times 10^6 \alpha_{xy}^{-2.888}$ and CO_2/CH_4 upper bounds using the formula $P_x = 5.369 \times 10^6 \alpha_{xy}^{-2.636}$ (where P_x is the permeability (barrer) of the most permeable x-gas and α_{xy} is the selectivity for the x/y gas pair).[6]

Concerning CO_2 separation membranes, according to the literature, their key drawback is the trade-off between high gas selectivity and separation efficiency. Building on the current research landscape, the latest advancements in CO_2 separation membranes are meticulously presented herein. Also, the challenges and future developmental trends in CO_2 separation membranes are explored in detail, presenting valuable reference and guidance for subsequent endeavors in the creation of novel CO_2 separation membranes.

[a]*College of Chemistry & Environmental Engineering, Yangtze University, Jingzhou, Hubei 434023, P. R. China. E-mail: yuweichu@126.com*

[b]*Hubei Engineering Research Centers for Clean Production and Pollution Control of Oil and Gas Fields, Jingzhou, Hubei 434023, P. R. China*

† Electronic supplementary information (ESI) available. See DOI: https://doi.org/10.1039/d4ra00444b

2. Mechanism of carbon dioxide membrane separation

With the development of technologies linked to polymer materials, technology known as the multi-component mixed gas membrane separation method has been gradually developed. When there is a concentration or pressure difference between two sides of the gas membrane as the driving force, the mixed gas can preferentially pass through it based on the difference in the rate of various gas components passing through the membrane. The fundamental membrane separation mechanisms are primarily split into the following three separation mechanisms because of the various membrane materials and properties.

2.1 Microporous diffusion

When a gas passes through a porous membrane, the gas molecules with different mixed components have different diameters, and thus the speed of passing through the membrane driven by the pressure discrepancy or concentration discrepancy is different. Small gas molecules pass through the membrane preferentially, while large gas molecules are difficult to pass through. The gas separation effect of porous membranes is mainly affected by the gas properties and membrane pore size.[7] Specifically, according to the membrane pore diameter, r, and the average diameter of the gas molecules, λ, the transfer mechanism of mixed gas in porous membranes can be classified into Knudsen diffusion, surface diffusion, capillary condensation, and molecular sieve diffusion,[8] as shown in Fig. 1.

2.2 Dissolution permeation diffusion

Different from the microporous diffusion mechanism of porous membranes, the process of gas passing through a dense membrane generally occurs as the following steps: firstly, the gas is adsorbed on the upstream side of the membrane and dissolved on the membrane surface; secondly, the gas diffuses within the membrane towards the downstream side due to concentration or pressure differences; and finally, the gas is released and desorbed on the downstream surface of the membrane (Fig. 2).[9] The dissolution diffusion mechanism, which realizes separation according to the difference between the amount of various gases dissolved in the membrane and their diffusion rate through the membrane, is the name given to this interpretation of gas permeation.

In the actual membrane separation procedure, the gas mixture passes through the membrane, but there is a difference in the speed at which the different gases pass through. After a multi-stage membrane separation process, the gas purity can be effectively increased through advancements in membrane separation technology, but this will also increase the energy consumption, limiting its potential for further commercial use.

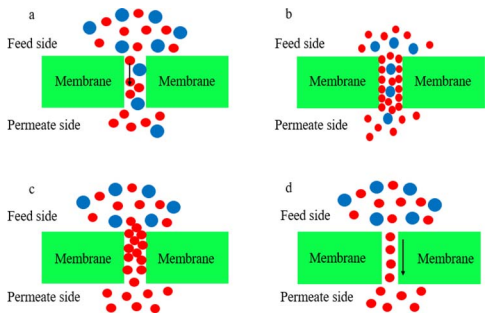

Fig. 1 Schematic diagram of the porous membrane transfer mechanism ((a) Knudsen diffusion, (b) surface diffusion, (c) capillary condensation, and (d) molecular sieve diffusion).

2.3 Facilitated transport

The mechanism of facilitated transport membranes was inspired by biofilms and has been extensively studied. Unlike the dissolution diffusion mechanism, there is a specific interaction between CO_2 and the functional groups in the facilitated transport membrane. Due to the reversible chemical reaction between the functional groups and CO_2, specific functional groups enhance the transport of CO_2 within the membrane.

The process of gas passing through facilitated transport membranes generally occurs as the following steps: at the feed-side interface of the membrane, CO_2 reacts with the carrier and forms a CO_2-carrier reaction product, which diffuses along its concentration gradient to the permeate side of the membrane. Due to the lower CO_2 partial pressure on the permeate side, CO_2 is released from the CO_2-carrier reaction product to the permeate side, while regenerating the carrier, which can then react with another CO_2 molecule on the feed side (Fig. 3). Therefore, other gases only undergo solution-diffusion, such as N_2, H_2, and CH_4.

The carriers of facilitated transport membranes can be small and mobile molecules, which are referred to as mobile carriers, or functional groups anchored on polymer backbones, the so-called fixed-site carriers. The fixed-site carrier can increase the membrane stability due to its polymeric nature and is inherently stable in the membrane. In addition, the mobile carrier may enhance the CO_2 flux due to its high mobility compared to the fixed carrier. Thus, a combination of fixed-site and mobile carriers should provide good membrane stability together with good CO_2 facilitation.[10]

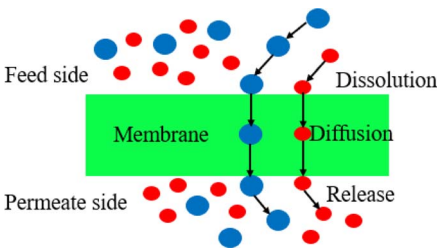

Fig. 2 Schematic diagram of solution permeation diffusion.

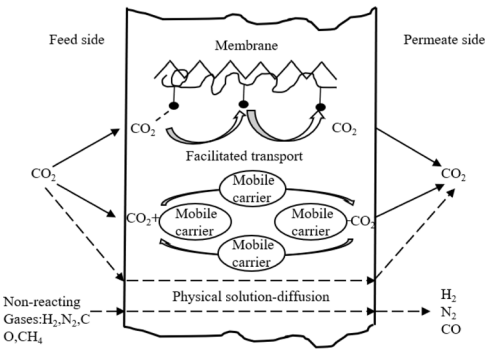

Fig. 3 Schematic diagram of the facilitated transport mechanism.[10]

3. Membranes for carbon dioxide separation

Membrane materials serve as the foundation of membrane separation technology, given that their performance directly impacts the potential applications of this technology. Gas separation membranes have a Robeson upper limit for permeability and selectivity, indicating that higher permeability results in lower selectivity, and *vice versa*. Therefore, in practical applications, membrane materials are selected based on the separation requirements, operating conditions and other relevant factors. Gas separation membranes can be classified into three groups including inorganic membranes, organic membranes, and emerging membranes.

3.1 Inorganic membranes

Membranes for gas separation that use inorganic materials as the separation medium are known as inorganic separation membranes. Inorganic membranes exhibit the benefits of superior chemical stability, controllable pore size distribution, *etc.* due to the characteristics of inorganic materials. Furthermore, the gas separation performance of inorganic membranes can be promoted by improving their pore size and structure. Compared with polymer organic membranes, some inorganic membranes such as graphene membranes have higher diffusion and selectivity. Some commonly employed CO_2 inorganic separation membranes include silica, zeolite, and graphene membranes.

3.1.1 Silica membranes. Uhlhorn *et al.*[11] first reported the use of an SiO_2 membrane for the separation of CH_4/CO_2 in 1989. They found that the typical SiO_2 membrane could readily adsorb water vapor on its surface, which may lead to the collapse of the structure of the SiO_2 membrane, reducing the effect of membrane separation. At present, there are two popular ways to increase the hydrothermal stability of SiO_2 membranes. One is to introduce hydrophobic groups in the membrane structure to improve its hydrophobicity, while the other is to introduce transition metals to strengthen the structural integrity of the membrane.[12]

Starting from the introduction of transition metals, Yan *et al.*[13] constructed cobalt-doped silica membranes by the sol–gel method, and explored the existing form of cobalt and the effect of the addition of cobalt on the pore structure and membrane separation performance. The findings demonstrated that the microporous SiO_2 membranes with 10% Co doping had a typical microporous structure, and the permeability of the Co-doped SiO_2 membranes to H_2 at 300 °C was 64.1 barrer and the H_2/CO_2 separation coefficient reached 6.61. Li *et al.*[14] selected several precursors and nickel sources to prepare nickel-doped silica membranes, and the CH_4 and CO_2 permeation fluxes of the Ni-doped SiO_2 membranes were 15.6 barrer and 6.4 barrer, respectively, and the CH_4/CO_2 separation factor was 2.43. Gu *et al.*[15] prepared aluminum-doped microporous SiO_2 membranes with tetraethyl orthosilicate and *sec*-butanol aluminum. After aging treatment for 500 h at 873 K and 16% water vapor, the H_2 passing rate of the aluminum-doped SiO_2 membranes changed slightly, while the hydrothermal stability was much higher than that of pure SiO_2 membranes.

There have been numerous investigations on enhancing the hydrothermal stability of SiO_2 membranes by adding hydrophobic groups. To obtain a hydrophobic SiO_2 membrane, Zhang *et al.*[16] used CTAB (cetyltrimethylammonium bromide), vinyl triethoxysilane and ethyl orthosilicate. The SiO_2 membrane had good permeability to CH_4 and CO_2, and the CH_4/CO_2 gas separation factor was 2.27 at a pressure difference of 20 kPa. Hong *et al.*[17] obtained a trifluoropropyl-modified SiO_2 membrane material and hydrophobically modified the ordinary SiO_2 membrane using trifluoropropyltrimethoxysilane. At 300 °C, the permeability of the membrane to H_2 was 47.7 barrer and the H_2/CO_2 separation coefficient reached 6.99.

Ding *et al.*[18] successfully prepared a heptadecafluorodecyl-modified SiO_2 membrane, and at 300 °C, the permeability of the membrane to H_2 was 100 barrer and the H_2/CO_2 separation coefficient reached 13.30. Compared with methyl, trifluoropropyl and other hydrophobic groups with relatively simple structures, the modification effect of heptadecafluorodecyl on the SiO_2 membrane was more obvious. The CO_2 separation performances of different silica membranes are summarized in Table 1. These are the best-performing membranes reported in the literature, and thus the selected values were chosen for inclusion in this table and the value in the subsequent tables are based on the same principle.

As can be seen in Table 1, most silica membranes were enhanced through the doping of transition metal ions and the introduction of hydrophobic groups. The efficacy of various transition metal ions in improving the gas separation performance of silica membranes varies. Notably, doping Co ions demonstrated superior effects compared to doping Ni ions. This discrepancy can be attributed to the presence of Co elements in Co-doped silica membranes, which existed in the form of Si–O–Co within the SiO_2 framework. In contrast, Ni-doped silica membranes incorporated Ni elements not only in the Si–O–Ni form in the SiO_2 framework but also filled some Ni and NiO crystals in the SiO_2 pores. This alteration in pore size compromised the gas separation performance of Ni-doped silica membranes compared to Co-doped silica membranes.[19]

The structural stability, pore size controllability, gas permeability and separation performance of SiO_2 membranes

Table 1 Gas separation performance of some silica membranes

Membrane	T (°C)	P (atm)	Permeability (barrer)	Selectivity
10% Co–SiO_2 membrane[13]	300	0.99	H_2: 64.1	CO_2/H_2: 6.61
10% Ni–SiO_2 membrane[14]	50	1.00	CO_2: 6.4	CO_2/CH_4: 2.43
0.04C-(0.9A-151) SiO_2 membrane[16]	75	0.20	CO_2: 13.4	CO_2/CH_4: 2.27
Trifluoropropyl–SiO_2 membrane[17]	300	0.99	H_2: 47.7	CO_2/H_2: 6.93
Heptadecafluorodecyl-modified SiO_2 membrane[18]	300	1.00	H_2: 100	CO_2/H_2: 13.30

can be effectively improved by doping transition metal ions and introducing hydrophobic groups for modification. Nevertheless, these two methods have certain drawbacks, where the pore size of the membrane material is easily changed by the metal ions by doping into the skeleton of the SiO_2 membrane, making it difficult to meet the requirements for gas separation. Furthermore, to date, the mechanism of the effect of hydrophobic group structure on the performance of SiO_2 membranes is unclear, which are still far from practical application.

3.1.2 Zeolite membranes. Since the 1990s, zeolite membranes have become a hot topic in membrane science research because of their specific space-oriented pore system, variable skeleton and other characteristics, which have the ability to produce effective molecule level separation.[20] They have been widely used in a variety of applications, including gas separation, isomer separation, and catalytic conversion.[21] In terms of CO_2 capture gas separation, zeolite membranes exhibit high selectivity for CO_2 adsorption due to their small pore structure,[22] potential high screening selectivity, and strong electrostatic field.[23]

Himeno *et al.*[24] prepared a DDR (deca-dodecasil R) membrane for CO_2 separation based on a zeolite membrane. At 25 °C, the permeability of the membrane to the CO_2 single component reached 100 barrer, and the selectivity of CO_2/CH_4 and CO_2/N_2 mixed gas with a 50/50 feed ratio was 200. Cui *et al.*[25] prepared a T-type zeolite membrane with strong CO_2 separation capability. At 70 °C, the optimal selectivity of the membrane for CO_2/CH_4 and CO_2/N_2 mixtures was 266 and 31, respectively. The 50/50 selectivity for CO_2/CH_4 and CO_2/N_2 at 35 °C was 400 and 107, respectively, indicating that the zeolite membrane has an excellent CO_2 separation performance. Gong[26] prepared a rhombic zeolite membrane *via* the secondary growth synthesis method. The ideal separation coefficient for the CO_2/N_2 single component and the separation coefficient of the two components reached 3.5 and 4.05, respectively. With an increase in temperature, the separation performance only decreased slightly and had good thermal stability.

Jang *et al.*[27] used the secondary growth method to synthesize OSDA (organic structure directing agent)-free CHA (chabazite) zeolite membrane. The maximum selectivity coefficient of the obtained CHA zeolite membrane for CO_2/N_2 was 12.5, indicating that the zeolite membrane has a good CO_2 separation performance. Kida *et al.*[28] synthesized a pure silica CHA zeolite (Si-CHA) membrane by using a porous α-alumina support and the results revealed that the Si-CHA membrane had ultra-high permeability, where at 25 °C and 0.1 MPa, the selectivity of the Si-CHA membrane for CO_2/CH_4 was as high as 130. Analogously, high-quality Si-CHA zeolite membranes were prepared using a green and fluorite-free synthesis route by Zhou *et al.*,[29] where the best membrane displayed a CO_2 permeability of 120 barrer and CO_2/CH_4 selectivity as high as 480 for an equimolar CO_2/CH_4 gas mixture at 25 °C and 0.2 MPa pressure drop.

Yu *et al.*[30] successfully prepared a CHA nanocrystalline membrane by adding fluoride. The addition of fluoride increased the permeability and separation performance of the CHA nanocrystalline membrane and increased the selectivity for CO_2/CH_4 to 32. The Y-type zeolite membrane with CO_2/N_2 selectivity of up to 500 prepared by Jeremy *et al.*[31] had high CO_2 selectivity, but low CO_2 permeability. The CO_2 separation performances of different zeolite membranes are reported in Table 2.

Based on the information in Table 2, it is evident that the selectivity and permeability of Si-CHA zeolite membranes surpass that of ordinary zeolite membranes (T/Y type). This superiority can be attributed to the unique and regular crystalline pores of Si-CHA zeolite membranes and their adjustable skeleton silicon–aluminum ratio (molar ratio of membrane skeleton silicon element to aluminum element). The pore size of Si-CHA zeolite membranes is larger than that of water molecules, H_2 molecules, and CO_2 molecules, but smaller than that of most gas molecules. This characteristic endows Si-CHA zeolite membranes with the potential for high molecular sieving selectivity, enabling them to achieve elevated permeability and selectivity.[32]

CHA-type zeolite membranes demonstrated an attractive separation performance for most studied applications. The two major contributing factors are as follows: CHA-type zeolite membranes (1) are more mature and (2) have three-dimensional channels and a suitable pore size. Preventing zeolite growth inside porous substrates and reducing the membrane thickness are effective strategies for improving the membrane permeance. In addition, it is important to conduct more membrane tests under close-to-realistic operating conditions, such as complex/real feed mixture and high operating pressure, to reveal the real-world performance for better assessment of the membrane potential.[33]

Zeolite membranes are beneficial for the adsorption and separation of CO_2 due to their small pore structure and strong electrostatic field. Nonetheless, adequate control of their microstructure and research into the mechanism for their

Table 2 Gas separation performances of some zeolite membranes

Membrane	T (°C)	P (atm)	Permeability (barrer)	Selectivity
DDR-type membrane[24]	25	1.97	CO_2: 30	CO_2/CH_4: 200
Zeolite T membrane[25]	35	0.99	CO_2: 46	CO_2/CH_4: 400
Chabazite membrane[26]	20	0.19	CO_2: 27	CO_2/N_2: 4.05
OSDA-free CHA membrane[27]	75	1.00	CO_2: 100	CO_2/N_2: 12.5
Si-CHA membrane[28]	25	0.99	CO_2: 400	CO_2/CH_4: 130
Si-CHA membrane[29]	25	1.97	CO_2: 120	CO_2/CH_4: 480
All-silica CHA nanocrystals membrane[30]	30	8.88	CO_2: 780	CO_2/CH_4: 32
Zeolite Y membrane[31]	30	1.36	CO_2: 9.6	CO_2/N_2: 503

generation remain significant barriers to their wider deployment. Therefore, high selectivity and high permeability remain key areas for zeolite membrane research.

3.1.3 Graphene membranes. Graphene materials were discovered to possess several advantages such as ultra-thin thickness, excellent mechanical strength, high temperature resistance, and good chemical stability. These attributes make them highly promising for the development of high-performance gas separation membranes. Recent research focused on two primary types of graphene membranes: layered graphene oxide membranes and graphene mixed matrix membranes.[34]

Jiang *et al.*[35] demonstrated that porous graphene can be used in gas separation from the perspective of first principles, and then designed and synthesized two types of porous graphene membranes and proved that atoms modified the porous edges had a great impact on the separation performance of the membranes. Wang *et al.*[36] designed and prepared a double-layer porous graphene membrane with a single-layer pore size of 2.5 nm, and by only shifting the relative position of the graphene layer, the effective pore size of the graphene membrane could reach 0.36 nm, which satisfies the technical specifications for the separation of CO_2, N_2 and CH_4. Celebi *et al.*[37] introduced nanopores in a CVD bilayer graphene structure by focused ion beam, with a size in the range of 10 nm to 1 μm. Among them, the permeability coefficient of the porous graphene membrane with a pore size of 7.6 nm for H_2 was much higher than that of the reported gas separation membranes and it had similar selectivity to H_2/CO_2.

Currently, porous graphene membranes are difficult to manufacture and puncture precisely, and their real gas selectivity is substantially lower than their theoretical selectivity.[38] The theoretical selectivity of graphene films surpasses their actual selectivity primarily due to the challenges in precisely controlling the interlayer spacing of graphene oxide films on the sub-nanometer scale using current technical methods. Consequently, the resulting graphene oxide films exhibit a non-uniform interlayer spacing, leading to an actual selectivity lower than the theoretical selectivity.

Therefore, researchers found that the nanoscale-thickness GO (graphene oxide) laminate films had excellent gas separation capabilities.

Kim *et al.*[39] created GO layered membranes *via* two distinct methods, and then studied how the micro-structure of the GO laminar membrane affected its ability to separate gases. It was found that GO membranes with a tightly packed microstructure had more complicated airflow channels and higher selective separation effects for CO_2/N_2 mixed gas. Li *et al.*[40] obtained an ultra-thin GO membrane with a thickness of 1.8 nm by vacuum filtration. The membrane exhibited high selectivity for H_2/CO_2 with a 3400 selectivity level due to the size sieving effect. Chi *et al.*[41] prepared GO nanosheets with a size of 13 μm and a complete structure. Based on this substance, GO membranes were assembled by various techniques. The selectivity factor for H_2/CO_2 was found to reach 240 in the GO membranes with more regular stacking structures, which had superior gas selectivity.

The preparation of large-scale, high-quality membranes remains a major challenge although GO layered membranes have significant advantages in the preparation of selective interlayer channels and high gas selectivity.[42] This is because different preparation methods have a significant impact on the gas selectivity of membranes. Therefore, researchers combined GO sheets with organic matter to improve the processability of the membrane.[43] The composite forms included GO sheets added to the membrane basal planes and filling organic matter or ionic liquid into the GO sheets.[44]

Xin *et al.*[45] modified GO nanosheets with sulfonated polymer molecular brushes and introduced GO sheets in a sulfonated polyetheretherketone (SPEEK) matrix to obtain graphene mixed matrix membranes. Further studies showed that the addition of sulfonated polymer-modified GO was beneficial to improve the CO_2 adsorption selectivity and diffusion selectivity of the membranes. Shen *et al.*[46] developed GO/PEBA (polyether block amide) mixed matrix membranes with various GO oxygen contents and studied the effect of oxygen content on the membrane separation performance. It was found that when the O/C ratio of GO was 0.55, the screening effect was strong and the gas separation performance was the best. The CO_2 permeability coefficient reached 97 barrer and the CO_2/N_2 selectivity reached 86. Shen *et al.*[47] used a vacuum spin coating method to fill polyethyleneimine (PEI) layer by layer between the GO film layers using the combined action of mechanical external forces and intermolecular forces to make the GO film microstructure more regular and orderly, and the H_2 permeability coefficient reached 840 barrer, with an H_2/CO_2 selectivity of 33. The CO_2 separation performances of different graphene membranes are summarized in Table 3.

Table 3 Gas separation performances of some graphene membranes

Membrane	T (°C)	P (atm)	Permeability (barrer)	Selectivity
GO layered membrane[39]	25	0.99	CO_2: 8500	CO_2/N_2: 20
Ultra-thin GO membrane[40]	20	1	H_2: 10	H_2/CO_2: 3400
GO nanosheets membrane[41]	25	0.99	H_2: 3400	H_2/CO_2: 240
Graphene oxide-doped ionic liquid membrane[44]	25	1	CO_2: 37	CO_2/N_2: 130
Graphene mixed matrix membrane[45]	25	0.99	CO_2: 1327	CO_2/N_2: 86.4
GO/PEBA membrane[46]	25	2.96	CO_2: 97	CO_2/N_2: 86
GO mixed matrix membrane[47]	25	1.97	H_2: 840	H_2/CO_2: 33

Referring to the data presented in Table 3, it is noticeable that the higher permeability observed in graphene oxide membranes is consistently correlated with lower selectivity. This phenomenon can be attributed to several factors. Firstly, in thicker gas separation membranes, the interaction between gas molecules and the channel walls tends to impede gas permeation. Additionally, longer permeation channels lead to increased collisions between mixed gas molecules, resulting in the transfer of linear momentum from lighter molecules to heavier molecules. This phenomenon generates collective flow, significantly reducing the separation efficiency of the membrane. However, by employing porous graphene thin films with atomic-level thickness, it became possible to enhance the selectivity and permeability by adjusting the pore structure (size), thereby greatly improving the efficiency of gas separation.[37]

3.1.4 Alumina-based ceramic membranes. In general, the mesoporous structure of alumina determines that the transport in alumina membranes occurs through the Knudsen diffusion mechanism. Due to the limited selectivity under this mechanism and the diffusion rate controlled by molecular weight, the application of alumina membranes in gas separation is restricted. Also, alumina is less suitable as a membrane material for mixtures such as CO_2/N_2 (with similar gas mass) and CO_2/H_2 (requiring selectivity for heavier components). Despite attempts to promote the surface diffusion of CO_2 through the modification of alumina membranes, success has been limited.[48] To achieve high separation factors in systems such as CO_2 and N_2, an interaction between one of the gases in the mixture and the membrane surface can be introduced by chemical modification of the separation layers. Some important works are presented below.

Cho *et al.*[49] reported the preparation of a modified γ-Al_2O_3 membrane by sol–gel coating with boehmite (AlOOH) sol. CaO was impregnated on the γ-Al_2O_3 membrane to improve the separation factor by introducing interactions between CO_2 gas molecules and the pore wall, but a high separation factor was not obtained. When the pressure ratio was 0.26, the separation factor was 1.72 at 298 K and 1.50 at 673 K. Kang *et al.*[50] synthesised γ-Al_2O_3 composite membranes modified with microporous silica layers to improve the separation factor of CO_2 to N_2, and the CO_2/N_2 separation factors through the silica-modified γ-Al_2O_3 membranes by dip-coating and pressurized coating from outside the support were about 2.4 and 1.45, respectively.

Isobe *et al.*[51] prepared an AlOOH/Al_2O_3 porous ceramic membrane, with the porous Al_2O_3 bodies having an average pore size of approximately 74 nm and porosity of 40.4%, and the CO_2/N_2 gas selectivity was approximately 0.8 at 0.04 MPa. Carbon dioxide separation using an α-alumina ceramic tube-supported cellulose triacetate–tributyl phosphate composite membrane was reported by Shankar *et al.*,[52] and the CO_2 permeability coefficient could reach 4248 barrer, with a CO_2/N_2 selectivity of 0.84.

Sharma *et al.*[53] prepared an asymmetric graded membrane substrate comprised of a macroporous industrial alumina-based ceramic support with a systematic graded assembly of sol–gel derived γ-alumina intermediate and silica–CTAB sublayer-based multilayered interface. The ceramic membrane exhibited the optimum CO_2 permeance of 599 barrer with CO_2/N_2 selectivity of 12.5 at 80 °C under a trans-membrane pressure drop of 0.8 bar. The CO_2 separation performances of different alumina-based ceramic membranes are summarized in Table 4.

It can be seen that the gas selectivity of alumina membranes is low in Table 4 because the mesoporous structure of alumina determines that the transport in the membrane occurs through the Knudsen diffusion mechanism. Due to the limited selectivity under this mechanism and the diffusion rate controlled by molecular weight, the application of alumina membranes in gas separation is restricted. Although some alumina membranes have high gas permeability, the development of alumina membranes should still aim to improve their selectivity for gas separation.

Considering their narrow and controllable pore size distribution, excellent gas selectivity and permeability, high temperature resistance and high pressure capabilities, inorganic membranes are well suited for the separation of CO_2. However, due to certain characteristics of inorganic materials such as high brittleness and low elasticity, the fabrication of inorganic membranes is challenging, and thus their application in the field of gas separation is limited.[54]

3.2 Organic membranes

In addition to inorganic membranes, organic membranes are currently receiving significant research attention. Furthermore, numerous organic membranes have been applied,

Table 4 Gas separation performances of some alumina-based ceramic membranes

Membrane	T (°C)	P (atm)	Permeability (barrer)	Selectivity
γ-Al_2O_3 composite membranes[50]	25	2.96	CO_2: 28.56	CO_2/N_2: 2.4
$AlOOH/Al_2O_3$ porous ceramics membrane[51]	79	0.39	—	CO_2/N_2: 0.8
α-Alumina ceramic tube-supported cellulose triacetate–tributyl phosphate membrane[52]	30	1.97	CO_2: 4248	CO_2/N_2: 0.84
Industrial alumina-based ceramic substrate amino silicate membrane[53]	80	0.79	CO_2: 599	CO_2/N_2: 12.5

demonstrating good gas separation performances and mechanical properties. The commonly used organic materials include cellulose, polyamide, polysulfone, and polyether.

3.2.1 Cellulose membranes. Cellulose is a naturally occurring polymer that is abundant in nature, easily accessible, and biodegradable. On the premise of environmental protection, cellulose and its derivatives have good selectivity for O_2, N_2 and other gases due to their multi-hydroxyl structure and intermolecular hydrogen bonds. Therefore, cellulose and its derivatives, primarily ethyl cellulose, cellulose acetate and derivatives, were the first organic membrane materials to be created and used.[55]

In 1982, Dow Chemical Company developed a separation membrane based on cellulose triacetate and industrially applied it in 1983. Its industrial operation effect was obvious. This membrane material was discovered to have strong plasticization resistance, and simultaneously poor temperature resistance. Hao *et al.*[56] prepared a cellulose acetate separation membrane by the wet phase conversion method, which could achieve a high CO_2 transmission rate without heat treatment. Wu *et al.*[57] prepared a cellulose membrane by directly dissolving natural cellulose, and the wet cellulose membrane exhibited strong permeability to acidic gases such as CO_2. At 25 °C, the permeability of the membrane to CO_2 was 120 barrer. The ideal separation factors of mixed gas systems containing CO_2/H_2 and CO_2/N_2 were 15 and 50, respectively, showing a good selective separation performance. Jie *et al.*[58] chose cellulose/NMMO (*N*-methylmorpholine-*N*-oxide)/water ternary spinning as a membrane system to obtain a dense cellulose hollow fiber membrane. At 25 °C and 0.5 MPa, the membrane had a CO_2 permeation rate of 750 barrer and the ideal separation factors of the mixed gas systems containing CO_2/N_2 and CO_2/CH_4 were 45 and 30, respectively.

Ansaloni *et al.*[59] studied a cellulose nanofiber membrane and found that it had good selectivity for CO_2/N_2 and CO_2/CH_4 mixed gases, but the flux of CO_2 was low. Subsequently, a composite membrane was obtained by combining the cellulose nanofiber membrane with polyvinyl amine, and the membrane flux of CO_2 was improved to a certain extent. When monoglycol and triethylene glycol were combined with a cellulose triacetate (CTA) membrane, Lu *et al.*[60] discovered that the permeability of the membrane to CH_4 and CO_2 increased. The reason for this may be that the free volume of the cellulose membrane increased after treatment with an alcohol solution, which was more conducive to gas diffusion. Shang *et al.*[61] investigated the gas separation performance of a ethyl cellulose homogeneous membrane by structural modification and solvent optimization. It was found that the separation factors of the ethyl cellulose homogeneous membrane for O_2/N_2 and CO_2/N_2 reached 6.2 and 33.0, respectively, demonstrating significantly high CO_2 selectivity. The CO_2 separation performances of different cellulose membranes are summarized in Table 5.

It is notable that the cellulose/NMMO/water membrane exhibited remarkable selectivity and permeability, as shown Table 5. This can be attributed to several factors. Firstly, the wet method employed for the preparation of the homogeneous and non-porous cellulose hollow gas separation membrane ensured a dense structure after natural drying, which initially did not exhibit significant gas permeability. However, upon humidification, water infiltrated the amorphous regions of cellulose, forming a "water channel". The gas molecules dissolved and diffused within this "water channel", facilitating their permeation and separation. Consequently, the water content played a crucial role in determining the gas permeation rate. Notably, CO_2 demonstrated high solubility in water, leading to enhanced permeability in the membrane post-water swelling. This phenomenon resulted in high ideal separation factors for N_2, CH_4, and even H_2.[58]

Although cellulose and its derivatives have been employed as membrane materials for the longest time and demonstrated a strong CO_2 separation performance in the actual usage process, the current utilization of the maximum value of cellulose materials remains on the first-order derivatization. Thus, future research on cellulose gas separation membranes should focus on further modifying and preparing secondary, tertiary and other multi-level derivatives.

3.2.2 Polyimide membranes. To solve the shortcomings of cellulose membrane materials such as poor temperature resistance, researchers found that polyamide, polyimide and their derivatives have good advantages such as high temperature resistance and chemical resistance, and thus potential to be used for the preparation of CO_2 separation membranes. At present, some commercial polyimide membranes already exist, such as Upilex, Kapton, and Matrimid® 5218 membranes. However, although these polyimide membranes show excellent CO_2 separation performances, their CO_2 permeability still lags behind the upper limit of Robeson 2008. In addition, the physical aging of polymer materials is also a problem that needs to be overcome in polyimide films.

Physical aging of polymer materials refers to the alteration of their appearance, physical properties, mechanical properties, and electrical properties when exposed to environmental conditions such as light, oxygen, and heat. Physical aging

Table 5 Gas separation performances of some cellulose membranes

Membrane	T (°C)	P (atm)	Permeability (barrer)	Selectivity
Cellulose acetate separation membrane[56]	25	4.93	CO_2: 520	CO_2/CH_4: 12
Cellulose membrane[57]	25	5.92	CO_2: 120	CO_2/N_2: 50
Cellulose/NMMO/water membrane[58]	25	4.93	CO_2: 750	CO_2/N_2: 45
Cellulose nanofiber membrane[59]	35	0.99	CO_2: 340	CO_2/N_2: 35
Cellulose triacetate membrane[60]	35	7.4	CO_2: 7.2	CO_2/CH_4: 28
Ethyl cellulose homogeneous membrane[61]	30	0.99	—	CO_2/N_2: 33

directly impacts the gas separation performance of polymer membranes. Following physical aging, the permeability of the membrane to CO_2 typically increases significantly, while the selectivity for CO_2 over other gases in a mixed gas decreases, resulting in a diminished gas separation effect.[62]

Thus, to enhance the CO_2 permeability of polyimide membranes, researchers typically modify their manufacturing procedures. It was found that the introduction of sterically hindered groups or twisted structures in the polymer backbone can weaken or eliminate the accumulation of polymer chains and effectively improve the permeability of the polymer.[63]

Sysel *et al.*[64] introduced the –$(CF_3)_2$– group in polyimide to prepare modified polyimide membranes for the separation of CO_2/CH_4 mixed gas. It was found that the separation coefficient of the modified polyimide membrane for the CO_2/CH_4 system reached 51. Fang *et al.*[65] prepared a 6FDA-type polyimide separation membrane. At 35 °C and 101.3 kPa, the CO_2 permeability coefficient of the membrane was 65 barrer and its ideal separation factor was 30. Maya *et al.*[66] introduced ethylene oxide in the polyimide framework by copolymerization. After heating to 200 °C, the CO_2 permeation rate of the modified polyimide membrane increased from 23.87 barrer to 57.25 barrer, but as the permeation rate increased, the selectivity of the membrane to gas was reduced by 10%. Zhang *et al.*[67] prepared two types of polyimide membranes without –CF_3– groups and with –CF_3– groups, respectively. Following a performance comparison, it was found that the introduction of the –CF_3– group enhanced the permeation rate of CO_2 from 18 barrer to 1858 barrer, but the selectivity coefficient for CO_2/CH_4 decreased from 31.3 to 18.9.

Zhu[68] prepared 9FDA (fluorinated dianhydride aromatic) polyamide by aniline and 9-fluorenone. Under the condition of 25 °C and 101.3 kPa, the separation coefficient of CO_2/N_2 was 26.65, and the separation coefficient of CO_2/CH_4 was 22.70, showing good selectivity. Si *et al.*[69] synthesized polyimide membranes with 4,4′-diamino diphenyl ether, 4,4′-diamino diphenylmethane and 3,3′,4,4′-benzophenone tetracarboxylic dianhydride as monomers. CO_2/CH_4 exhibited a good gas separation performance and selectivity of 11.9. Eguchi *et al.*[70] used glycidyl to crosslink and modify polyimide to obtain a polyimide membrane. There was a good balance between CO_2/CH_4 selectivity and CO_2 permeability. After crosslinking and modification, the CO_2 permeability of the polyimide membrane decreased from 150.5 barrer to 94.6 barrer, but its selectivity increased from 27.5 to 32.7. The CO_2 separation performances of different polyamide membranes are summarized in Table 6.

The data presented in Table 6 reveals that the polyethylene oxide-containing copolymer membrane exhibited superior selectivity. This can be attributed to its composition, which included flexible polyethylene oxide (PEO) segments and rigid polyimide segments. PEO possesses strong affinity for CO_2, thereby enhancing the gas selectivity of the membrane.[66] Additionally, decarboxylation cross-linking of polyimide membranes improved their permeability. This process involved a thermally induced reaction that increases the polymer spacing of the polyamide membrane, nearing the estimated distance between cross-linked polymer chains, and consequently enhancing the membrane permeability.[67] Notably, polyimides show no CO_2-induced plasticization phenomenon even at pressures of up to 30 atmospheres.

Despite the fact the current research shows that polyimide and its derivative membrane materials have the benefits of high permeability and good separation performance and good application prospects in the field of CO_2 gas separation, the further application of polyamide membranes is hindered by challenges such as their susceptibility to physical aging and complex preparation process.

3.2.3 Polysulfone membranes. During the study of polymer gas separation membranes, researchers found that polysulfone contains alkyl–sulfone–aryl chain segments in its structure. Materials such as bisphenol A polysulfone, polyarylsulfone, and polyethersulfone, which are derived from polysulfone, have potential to serve as effective gas separation materials due to their favorable film-forming characteristics and gas selectivity. However, it has been observed that polysulfone membranes, such as polyimide membranes, exhibit poor gas permeability. Consequently, current research on polysulfone materials primarily focuses on modifying polysulfone or developing composite membranes to enhance the gas separation performance.

Zhang[71] synthesized a fluorine-containing polysulfone membrane by polycondensation reaction and compared its performance with that of a commercial polysulfone membrane. It was discovered that the polysulfone membranes containing fluorine had a greater gas permeability coefficient. Additionally, a hybrid membrane was created by dispersing multi-walled nanotubes in a matrix made of fluorine-containing polysulfone. The permeability coefficient for CO_2 gas was 12.73

Table 6 Gas separation performances of some polyamide membranes

Membrane	T (°C)	P (atm)	Permeability (barrer)	Selectivity
Modified polyimide membrane[64]	25	0.99	CO_2: 8.06	CO_2/CH_4: 51
6FDA-type polyimide membrane[65]	35	1	CO_2: 65	CO_2/N_2: 30
Polyimide framework membrane[66]	30	3	CO_2: 57.25	CO_2/N_2: 54.52
Polyimide membrane[67]	35	2	CO_2: 1858	CO_2/CH_4: 18.9
9FDA polyamide membrane[68]	25	1	CO_2: 12.26	CO_2/N_2: 26.65
Polyimide membrane[69]	25	1	CO_2: 1.19	CO_2/CH_4: 11.9
Polyimide membrane[70]	35	4.42	CO_2: 150.5	CO_2/CH_4: 27.5

barrer at a pressure of 1 atm and temperature of 25 °C, and the selectivity coefficient was 28.9, which are 19% and 5.5% higher than that of the undoped fluorine-containing polysulfone membrane, respectively.

He[72] synthesized a PSF (polysulfone)/PDMS (polydimethylsiloxane) copolymer membrane. Under the conditions of 1 atm and 55 °C, the permeability coefficients of the PSF–PDMS 10% membrane for CO_2 and CH_4 were 73.7 barrer and 17.6 barrer, respectively, while its selectivity coefficient for a CO_2/CH_4 mixture was 4.2, showing a good gas separation performance. Shahid *et al.*[73] prepared a mixed matrix membrane using PI, PSF, and ZIF-8. When 30 wt% ZIF-8 was added, the CO_2 permeability of the mixed matrix membrane was 136% higher than that of the PI (polyimide)/PSF (polysulfone) membrane. The selectivity coefficient for CO_2/CH_4 was not much different from that of the PI/PSF membrane. Mannan *et al.*[74] studied the CO_2/CH_4 separation performance of a blend membrane based on polysulfone/polyethersulfone and found that the addition of polyethersulfone (PES) significantly improved the separation performance of the blend membrane for the CO_2/CH_4 mixed system.

Meng *et al.*[75] prepared a series of mixed matrix membranes employing graphene oxide, carbon nanotubes, and polysulfone. Compared with the pure polysulfone membranes, the CO_2 permeability coefficient of the mixed matrix membranes increased by as much as 422 barrer, indicating that the presence of carbon nanotubes significantly improved the CO_2 permeability. Meng *et al.*[76] selected PAF-56P (porous aromatic framework) as the separation medium to prepare a PAF-56P/PSF composite hollow fiber membrane, which showed good CO_2 permeability in the process of CO_2/N_2 separation. The separation coefficient of the CO_2/N_2 mixed system reached 38.9 and the membrane permeability reached 93–141 barrer, with strong gas separation ability. The CO_2 separation performances of different polysulfone membranes are summarized in Table 7.

The data in Table 7 demonstrate that the PI/PSF/ZIF-8 membrane exhibited the highest gas selectivity. This can be attributed to the porous structure, high specific surface area, and molecular sieving characteristics of ZIF-8. These features are expected to enhance the separation performance of the blend polymer membrane, while the presence of PI/PSF would increase the resistance of the system to plasticization.[73] Furthermore, polysulfone mixed matrix membranes demonstrated improved gas permeability. The use of *N*,*N*-dimethylformamide as a solvent for polysulfone and a dispersant for inorganic filler particles proved to be effective. Additionally, the incorporation of graphene oxide and carbon nanotubes significantly enhanced the hydrophilicity of the membrane. This facilitated the permeation of CO_2, given its high solubility in water, thereby improving the membrane permeability.[75]

Polysulfone membranes usually have good film forming properties, outstanding processing properties, excellent mechanical strength and good thermal stability. Furthermore, the separation membranes prepared using polysulfone and its derivatives have the advantages of uniform micropores and high porosity, and are popular for fluid separation. Polysulfone separation membranes will play a crucial role in gas separation for the foreseeable future.

3.2.4 Polyether membranes. Recent studies on membrane materials have shown that ether oxygen (EO) groups have a unique 'dipole–quadrupole' effect on CO_2, which can promote the dissolution rate of CO_2 in membrane materials to some extent and increase the permeation rate of CO_2. Therefore, research also focused on polyether or block polyether as gas separation membrane materials.

Zhou *et al.*[77] prepared a polyionic liquid-reinforced block polyether (F127/PIL) semi-interpenetrating network membrane. It was found that when the mass ratio of F127 to PIL was 30 : 70, the tensile strength of the F127/PIL semi-interpenetrating network membrane reached the maximum of 4.569 MPa.

Table 7 Gas separation performances of some polysulfone membranes

Membrane	T (°C)	P (atm)	Permeability (barrer)	Selectivity
Polysulfone membrane[71]	25	1	CO_2: 12.73	CO_2/CH_4: 28.9
PSF/PDMS membrane[72]	55	1	CO_2: 73.7	CO_2/CH_4: 4.2
PI/PSF membrane[73]	35	4.93	CO_2: 20	CO_2/CH_4: 42
PSF/PES membrane[74]	25	5.92	CO_2: 22.5	CO_2/CH_4: 6.5
Mixed matrix membrane[75]	25	0.99	CO_2: 975	CO_2/N_2: 1.94
PAF-56P/PSF membrane[76]	25	1	CO_2: 141	CO_2/N_2: 38.9

Wang *et al.*[78] selected polyether copolyamide Pebax1074 as the main membrane material to prepare a PSF/PDMS/Pebax1074 gas separation membrane with an ultrathin separation layer. It was discovered that the gas penetration flow in the membrane decreased significantly with an increase in the concentration of Pebax1074 on the membrane material, but the gas selectivity gradually increased.

Zhao *et al.*[79] used two different polyether copolyamides (highly selective Pebax1657 and highly permeable Pebax2533) to prepare gas separation membranes. It was found that the higher the polyether content in the blend membrane, the greater the CO_2 and N_2 permeability coefficients; conversely, the CO_2/N_2 selectivity decreased as the polar ether bond concentration increased. Car *et al.*[80] prepared a mixed membrane by blending polyethylene glycol (PEG) and Pebax1657. Compared with the pure Pebax1657 membrane, the cross section of the mixed membrane was more regular and orderly. When the performance of gas separation was examined, it was discovered that the CO_2/N_2 selectivity of the mixed membrane remained unchanged, while its CO_2 permeability coefficient doubled.

Further, Reijerkerk *et al.*[81] blended PEG, Pebax1657 and polydimethylsiloxane (PDMS) to prepare a mixed membrane. The CO_2/N_2 selectivity of the combined membrane was lower than that of the pure Pebax1657 membrane, but its CO_2 permeability was five times higher. Xiao *et al.*[82] prepared a polyimide film containing PPO segments by polymerization and studied its gas separation performance. It was found that with an increase in PPO content, the separation coefficient for CO_2/N_2 increased from 18.77 to 30.12, which indicated that the introduction to PPO segments had a significant effect on the gas separation performance of the membrane material. The CO_2 separation performances of different polyether membranes are summarized in Table 8.

It was evident that the polyethylene glycol (PEG)/Pebax1657/polydimethylsiloxane (PDMS) membrane exhibited high gas permeability according to Table 8. This can be primarily attributed to the presence of PDMS in the membrane structure, which enhanced the permeability to CO_2 due to its large free volume.[81] Additionally, polyether copolymer membranes demonstrated relatively high gas selectivity. This was mainly due to the low concentration of polar ether bonds present in the polymer membrane. The selectivity of polyether-based CO_2/N_2 separation membranes predominantly relied on their dissolution selectivity. Thus, as the concentration of polar groups in the polymer matrix decreased, the CO_2/N_2 selectivity of the membrane generally decreased, while it increased with a decrease in the concentration of polar ether bonds.[79]

Studies indicated that the incorporation of polyether or block polyether in other polymers is an effective method for enhancing the gas separation capabilities of polyether membranes. This approach can effectively regulate the microstructure and separation performance of the membranes. Nonetheless, the widespread adoption of polyether membrane materials has been impeded by their complex preparation process and susceptibility to fouling, thus restricting their current utilization primarily to indoor research.

The organic membranes prepared using cellulose, polyamide, polysulfone, polyether and other polymer materials have good separation ability and good application prospect for CO_2. However, the majority of organic membranes exhibit the problems of poor anti-pollution and poor mechanical properties, which have a direct impact on their service life and CO_2 separation effect,[83] further restricting the application of organic membranes in the field of CO_2 gas separation.

3.3 Emerging membranes

As research into separating membrane materials is progressively becoming more in-depth, an increasing number of innovative membrane materials have been developed, among which, the most well-known are composite membranes, MOF membranes, ZIF membranes, CMS membranes, PIM membranes and facilitated transport membranes.

3.3.1 Composite membranes. As already noted, although organic membrane materials have a greater CO_2 separation effect, inorganic membrane materials offer better chemical stability, thermal stability and gas selectivity. Thus, to create an inorganic–organic composite membrane that has the benefits of easy processing and the high mechanical properties and thermal stability of inorganic membranes, researchers attempted to combine inorganic materials with organic materials. This type of membrane has promising application possibilities.[84]

The inorganic materials that are frequently utilized for the preparation of composite membranes include zeolite molecular sieves,[85] metal–organic frameworks[86] and carbon nanotubes.[87]

Table 8 Gas separation performances of some polyether membranes

Membrane	T (°C)	P (atm)	Permeability (barrer)	Selectivity
F127/PIL membrane[77]	30	1.18	CO_2: 155.59	CO_2/N_2: 24.16
PSF/PDMS/Pebax1074 membrane[78]	25	2.96	CO_2: 424	CO_2/N_2: 41.3
Polyether copolyamide membrane[79]	25	1.97	CO_2: 100	CO_2/N_2: 50
PEG/Pebax1657 membrane[80]	30	0.59	CO_2: 151	CO_2/N_2: 47
PEG/Pebax1657/PDMS membrane[81]	35	3.95	CO_2: 532	CO_2/N_2: 36.1
Polyether membrane[82]	35	0.99	CO_2: 131.61	CO_2/N_2: 30.12

Jiang *et al.*[88] introduced a zeolite thin layer into a PSF/Matrimid hollow fiber membrane and found that the selectivity for CO_2 in a CO_2/CH_4 mixed system was enhanced by 50%. Analogously, Wu *et al.*[89] prepared an improved mixed-matrix membrane (MMMs) by incorporating SAPO-34 zeolites as an inorganic material in the 6FDA–TrMPD (PI) polymer, and the CO_2 permeability of the 40 wt% SAPO-34 crystal-loaded MMMs increased from 751 to 1663 barrer, which corresponded to an increase of 121% compared with the neat 6FDA–TrMPD membrane (Fig. 4).

Muhammad *et al.*[90] explored the modification of NH_2–MIL-53, and then added it to CA (cellulose acetate) to prepare a composite membrane. The composite membrane had a CO_2 permeability of 52.6 barrer and CO_2/N_2 mixed system selectivity of 23.4, according to the gas separation performance test. Liu[91] used a PI/UiO-66–PEI–pSBMA membrane as the selective layer and polydimethylsiloxane (PDMS) as the intermediate layer to obtain a polyimide multilayer composite membrane. The addition of UiO-66–PEI–pSBMA increased the CO_2 permeation rate of the polyimide composite membrane by 129.34% and the selectivity for CO_2/CH_4 by 55.58%.

Li[92] prepared a TB (Troger's base)/NH_2–MIL-53(Al) hybrid membrane with a good gas separation performance successfully. During the mixed gas test, the CO_2 gas permeability of the membrane reached 308 barrer and the selectivity for CO_2/N_2 and CO_2/CH_4 mixed gas was 25.4 and 23.6, respectively. Gao[93] prepared a composite membrane by chemically adding amino siloxane GO to polyimide through chemical modification. The findings demonstrated that the solubility and thermal stability of the composite membrane were higher than that of the pure PI membrane and the CO_2 permeability increased from 8.93 barrer to 17.33 barrer, 20.10 barrer and 24.29 barrer, respectively. The CO_2 separation performances of different composite membranes are summarized in Table 9.

The data in Table 9 suggests that the 6FDA–TrMPD mixed matrix membrane demonstrated the highest permeability. This is attributed to the incorporation of the SAPO-34 molecular sieve inorganic material during the synthesis of the membrane. SAPO-34 molecular sieves serve as an effective material for inclusion in the polymer matrix, enabling the simultaneous screening of CO_2 from CH_4 and N_2, and thus enhancing the gas permeability. Additionally, in the aromatic polyimide containing 4,4′-(hexafluoroisopropylidene)diphthalic anhydride (6FDA), the introduction of a $-C(CF_3)_2-$ group restricted the torsional movement of the adjacent benzene rings and limited the dense packing of the polymer segments to some extent. This increased the free volume of the polymer and enhanced its gas permeation properties.[89]

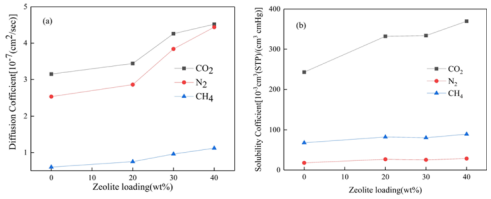

Fig. 4 (a) Diffusivity and (b) solubility of CO_2, N_2, and CH_4 in 6FDA–TrMPD/SAPO-34 MMMs with different zeolite loadings.[89]

The above-mentioned inorganic–organic composite membranes had obvious advantages in CO_2 selective separation; however, there are still some issues to be addressed. The interaction mechanism between the polymer and inorganic filler interface is not clear, inorganic fillers are difficult to disperse in the polymer matrix, they lack the foundation for large-scale manufacturing and application, and the CO_2 gas separation membranes still have a lot of room for improvement.

3.3.2 MOF membranes. In recent years, the utilization of MOF membranes in gas separation has emerged as a crucial area of research.[94] Recent investigations indicated that thin-film MOF membranes and MOF/polymer composite membranes outperform established polymer and zeolite membranes across various gas separation applications.[95]

Rui *et al.*[96] reported the preparation of a metal–organic framework membrane, MOF-1, and investigated its CO_2 separation performance. At feed pressures of 505 kPa and 298 K, the CO_2/CH_4 and CO_2/N_2 separation factors for the MOF-1 membrane were 328 and 410, respectively. The CO_2 permeability was measured at 255 barrer, demonstrating an excellent separation performance. Additionally, Chiou *et al.*[97] developed highly CO_2-selective metal–organic framework membranes, exhibiting outstanding CO_2 selectivity (ideal CO_2/N_2 selectivity of 42 and CO_2/CH_4 selectivity of 95). Among the available pure MOF membranes, this membrane also achieved the highest CO_2 permeability of approximately 500 barrer, with a CO_2/CH_4 selectivity exceeding 30.

Numerous studies explored the fabrication of mixed matrix membranes incorporating MOFs and other materials. Perez *et al.*[98] synthesized metal–organic framework 5 (MOF-5) nanocrystals with a high specific surface area and excellent thermal stability. These nanocrystals were added to Matrimid® to create a mixed matrix membrane for gas separation. Residual gas analysis of the permeate from mixed gases with varying ratios demonstrated an increase in CH_4 selectivity. Wang *et al.*[99] utilized porous ceramic alumina as a support and employed a solvothermal method to synthesize ZIF-62 polycrystalline MOF membranes *in situ*. They further prepared MOF glass membranes through a melt-quenching method, enhancing the molecular sieve separation capability through a glass transition treatment. The separation factors of the MOF glass membrane for H_2/CH_4, CO_2/N_2, and CO_2/CH_4 mixtures were measured to be 50.7, 34.5, and 36.6, respectively, significantly surpassing the Robeson upper limit.

Fu *et al.*[100] presented a novel approach by growing a metal–organic framework (MOF) on a covalent organic framework (COF) membrane to fabricate a COF–MOF composite membrane. The separation selectivity of this composite membrane for H_2/CO_2 mixed gas surpassed that of the individual COF and MOF membranes. Strong evidence supporting the synergistic effect between these two porous materials was observed in the COF–MOF composite membrane, which surpassed the Robeson upper limit for polymer membranes in H_2/CO_2 mixed gas separation. Similarly, in the pursuit of enhancing the gas permeability of ultra-microporous MOF

Table 9 Gas separation performances of some composite membranes

Membrane	T (°C)	P (atm)	Permeability (barrer)	Selectivity
Improved mixed-matrix membrane[89]	35	2.96	CO_2: 1663	CO_2/N_2: 14.8
NH_2–MIL-53(Al)/CA mixed matrix membrane[90]	25	2.96	CO_2: 52.6	CO_2/N_2: 23.4
PI/UiO-66–PEI–pSBMA membrane[91]	35	0.99	CO_2: 28	CO_2/CH_4: 56
TB/NH_2–MIL-53(Al) mixed matrix membrane[92]	35	3.95	CO_2: 308	CO_2/N_2: 25.4
Composite membrane[93]	30	0.99	CO_2: 17.33	CO_2/N_2: 30.58

membranes, Bu *et al.*[101] developed a COF/MOF all-nanoporous composite (ANC) membrane. This innovative approach involved doping a stable covalent organic framework (COF) with large and uniform pores (Fig. 5). In comparison to the original MOF membrane, the gas permeability of the COF/MOF membrane increased from 22 barrer to 551 barrer, with a slight decrease in selectivity. The CO_2 separation performances of different MOF membranes are summarized in Table 10.

Based on the data provided in Table 10, it is evident that the polycrystalline MOF membrane exhibited the highest permeability. This can be attributed to the preparation method involving the formation of a MOF glass membrane by melting and quenching the *in situ* solvothermal-synthesized polycrystalline ZIF-62 MOF membrane on a porous ceramic alumina carrier. During this process, the molten ZIF-62 phase infiltrated the nanopores of the carrier, thereby eliminating the intergranular defects formed in the resulting glass film. Consequently, the vitrification treatment significantly enhanced the gas permeability of the MOF membranes.[99]

In comparison to inorganic materials such as zeolites, MOFs exhibit distinct characteristics including high porosity, low density, ultra-high specific surface area, strong functionality, and precise size controllability, with pore sizes ranging from ultra-micropores to mesopores. Crucially, MOF materials offer facile functionalization and pore regulation through the alteration of metal ions and organic ligands, enabling tailored structural designs. The inherent attributes of high porosity, ultra-high specific surface area, and precise size controllability endow MOF materials with significant advantages over traditional inorganic porous materials, making them highly applicable in the field of gas separation membranes.[102]

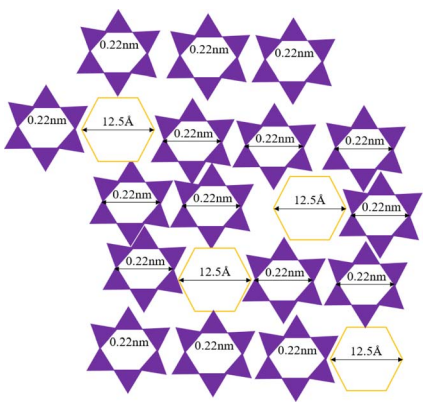

Fig. 5 Structure of COF-TpPa-1/ZIF-9 ANC membranes.[101]

The separation factor described in the MOF membrane section appeared to be comparable to that of the previously described inorganic membrane. This similarity is primarily due to certain shortcomings still present in MOF membranes, such as poor adhesion between the matrix and MOF layer, as well as defects at the filler–matrix interface, which ultimately reduce the selectivity of the membrane.

Although numerous MOF materials have been extensively studied, it is imperative to explore the untapped potential of MOFs in membrane gas separation applications.[103] The interplay between adsorption and diffusion, a topic seldom discussed, deserves attention. Additionally, it is necessary to underscore the significance of characterizing the gas distribution within MOFs. This understanding is crucial for unraveling the structure–property relationship governing gas adsorption and diffusion in MOF membranes.

3.3.3 ZIF membranes. Abundant research demonstrated the ease of synthesis, relative stability, and outstanding gas separation performance of ZIF membranes, presenting considerable potential for various innovative applications. However, challenges persist in their preparation and utilization, including issues of brittleness, cracking, repeatability, and process scalability.

Li *et al.*[104] successfully fabricated a zeolitic imidazolate framework (ZIF-7) molecular sieve membrane, exhibiting a promising mixture separation factor of 13.6 for H_2/CO_2 at 220 °C. This membrane demonstrated a commendable separation performance coupled with remarkable thermal stability. In the pursuit of enhanced membrane gas separation, Chang *et al.*[105] introduced amino-functionalized ZIF-7 (ZIF-7–NH_2), garnering attention for its pore-expanding structure post-complete removal of guest molecules (DMF). The ZIF-7–NH_2 membranes, synthesized with superior H_2 permeation flux and H_2/CO_2 selectivity compared to reported single-ligand ZIF-7 membranes, represent a significant advancement. The ZIF-7–NH_2 membrane effectively enhanced the separation performance of H_2/CO_2, closely approaching the upper limit of inorganic microporous membranes.

The synthesis of well-developed Co-based zeolitic imidazolate framework (ZIF) membranes on porous α-Al_2O_3 tubes presents considerable challenges. In a notable study by Liu *et al.*,[106] high-quality ZIF-9 membranes were successfully prepared, exhibiting remarkable H_2/CO_2 selectivity and thermal stability. The incorporation of 3-aminopropyltriethoxysilane

Table 10 Gas separation performance of some MOF membranes

Membrane	T (°C)	P (atm)	Permeability (barrer)	Selectivity
MOF-1 membrane[96]	25	4.98	CO_2: 255	CO_2/N_2: 410
CO_2-selective metal–organic framework membranes[97]	30	2.96	CO_2: 500	CO_2/N_2: 42
ZIF-62 polycrystalline MOF membrane[99]	25	0.99	CO_2: 2602	CO_2/N_2: 34.5
COF-TpPa-1/ZIF-9 membrane[101]	25	1.58	CO_2: 551	—

(APTES) as a covalent linker for α-Al_2O_3 tube modification contributed to the outstanding performance of the ZIF-9 membrane. The H_2/CO_2 mixture separation factor of the ZIF-9 membrane reached 21.5, surpassing the corresponding Knudsen coefficients significantly. In a related approach, Chang *et al.*[107] devised a hybrid metal zeolitic imidazolate framework membrane by introducing zinc ions and cobalt ions in the ZIF structure. The research findings highlighted the superior H_2/CO_2 separation factor of the hybrid metal ZIF membrane, which is attributed to its exceptionally high specific surface area.

To facilitate the widespread industrial implementation of ZIF membranes, significant efforts have been devoted to their preparation and support. A continuous ZIF-8 membrane was successfully synthesized on the outer surface of silicon nitride hollow fibers using a one-step hydrothermal method.[108] This approach achieved an H_2/CO_2 separation factor of 11.67, which was attributed to the robust CO_2 adsorption capabilities of the ZIF-8 structure. In a related study, Jia *et al.*[109] developed ZIF-8@cellulose nanofiber (ZIF-8@CNF) composite membranes. These membranes were created through the *in situ* growth of ZIF-8 crystals on cellulose nanofibers (CNFs) using a vacuum filtration process. The resulting membrane exhibited a CO_2 permeability of 550 barrer, with the ideal selectivity for CO_2/N_2 and CO_2/CH_4 reaching 45.5 and 36.2, respectively.

Taking inspiration from the adhesive properties of marine mussels, Nguyen[110] investigated the gas separation performance of a ZIF-8 membrane synthesized on a polydopamine-functionalized stainless-steel mesh (SSNs). In single-component gas permeation tests (Fig. 6), the PDA-functionalized ZIF-8 membrane demonstrated separation abilities for CO_2/N_2, H_2/N_2, and H_2/CO_2 with selectivity values of 1.25, 4.30, and 3.44, respectively. Under the optimal conditions, the efficiency of the 0.2 M material solution for H_2/CO_2 was maximized at 11.3.

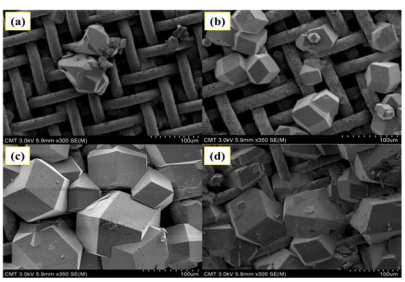

Fig. 6 FESEM images of ZIF-8 layers prepared on PDA-functionalized SSNs with different synthesis times: 8 h (a), 16 h (b), 24 h (c), and 48 h (d).[110]

Building on the preparation of ZIF-8 membranes, researchers have enhanced the membrane separation performance through structural regulation.[111] In a study by Lang,[112] the replacement of methylimidazole (MeIM) with 5,6-dimethylbenzimidazole (DBIM) through membrane surface ligand exchange (MSLE) was explored, assessing its impact on the gas separation performance of ZIF-8 membranes with different intergranular defects (perfect and imperfect membranes). The results revealed a significant improvement in membrane selectivity, which was primarily attributed to the reduction in intercrystallite pore diffusion rate resulting from the short-term ligand exchange. This reduction was more pronounced for larger molecules than smaller molecules, leading to a decrease in gas permeability and increase in separation factor. The CO_2 separation performances of different ZIF membranes are summarized in Table 11.

As indicated in Table 10, the ZIF-8@CNF membranes exhibited the highest selectivity and permeability. This enhancement can be attributed to the preparation method involving the synthesis of ZIF-8@cellulose nanofiber (ZIF-8@CNF) composite membranes through the *in situ* growth of ZIF-8 crystals on CNFs *via* vacuum filtration. The electrostatic forces between –COO– of CNFs and Zn^{2+} of ZIF-8 facilitated the homogeneous anchoring of ZIF-8 crystals on CNFs. As the loading of ZIF-8 increased sufficiently, the intrinsic selectivity of ZIF-8 significantly contributed to the gas separation.[109]

However, despite their advantages of easy synthesis and good stability, ZIF membranes are associated with challenges in the competitive separation of H_2 and CO_2, together with concerns about their mechanical strength under high pressure.[113] Future research on ZIF membranes should prioritize enhancing the separation selectivity of H_2 and CO_2, while addressing the mechanical strength challenges associated with high-pressure applications.

3.3.4 CMS membranes. CMS membranes, derived from the pyrolysis of polymer precursors, exhibit an ultra-microporous structure capable of separating small gas pairs with minimal diameter differences. They demonstrate superior gas permeability and selectivity compared to polymer membranes. However, the gas permeability of conventional pure CMS membranes cannot satisfy commercial application requirements due to their disordered pore structure and high molecular diffusion resistance. The incorporation of functional materials in membrane precursors to create hybrid CMS

Table 11 Gas separation performance of some ZIF membranes

Membrane	T (°C)	P (atm)	Permeability (barrer)	Selectivity
ZIF-7–NH_2 membrane[105]	25	0.99	CO_2: 60	CO_2/H_2: 19
ZIF-9 membrane[106]	25	0.99	CO_2: 52.3	CO_2/H_2: 21.5
Hybrid metal ZIF membrane[107]	55	0.99	CO_2: 54	CO_2/H_2: 14.1
ZIF-8@CNF membrane[109]	25	2.96	CO_2: 550	CO_2/N_2: 45.5
ZIF-8 membrane[110]	35	0.99	—	CO_2/H_2: 11.32

membranes has been recognized as an effective strategy for adjusting the disordered pore structure of traditional pure CMS membranes, consequently significantly enhancing their permeability.[114]

Numerous studies have explored the incorporation of polyether or polyimide in membrane precursors to develop CMS membranes. Wang *et al.*[115] synthesized a CMS membrane using carboxylated polyimides with various 6FpDA : DABA molar ratios. The resulting CMS membrane, which was pyrolyzed at 576 °C, exhibited CO_2 and C_2H_4 permeabilities of 3573 and 244.6 barrer, with CO_2/CH_4 and C_2H_4/C_2H_6 ideal selectivity of 51.5 and 4.80, respectively. Similarly, Hou *et al.*[116] produced CMS membranes with a high CO_2 separation performance through the pyrolysis of hydroxy-containing polyetherimide (BAHPPE–6FDA-type HPEI) precursors. The structural properties were found to significantly influence the carbon and pore structures, as well as the CO_2 separation performance (Fig. 7). The CMS membrane demonstrated a relatively high CO_2 permeability of approximately 10 000 barrer and enhanced CO_2/N_2 (or CH_4) selectivity was achieved after 60 days of aging under vacuum.

Pérez-Francisco *et al.*[117] presented a CMS membrane derived from dense membranes composed of a blend of a rigid polyimide (PI) DDPD–IMM and polybenzimidazole (PBI). The CMS membrane derived from the pure PI DPPD–IMM membrane exhibited the highest permeability coefficients (P_{CO_2} = 503 barrer) and the highest separation factors ($\alpha CO_2/CH_4$ = 56.5). The results suggested that increasing the concentration of PI in the membrane blend precursors positively influenced the permeability, diffusion coefficients, and selectivity of the CMS membranes. Similarly, Shin *et al.*[118] introduced a novel methodology for achieving a high separation performance in CMS fiber membranes by uniformly integrating double-stranded polysilsesquioxanes in the polyimide matrix. This innovative CMS membrane exhibited a substantially improved CO_2 permeability by up to 546% compared to its precursor fiber analogues. Furthermore, a poly(dimethylsiloxane) coating delayed physical aging, maintaining a high CO_2 permeability of 354 barrer with a CO_2/CH_4 selectivity of 56.

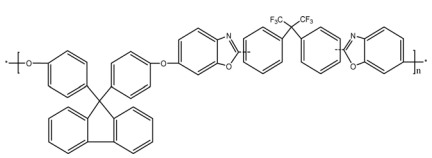

Fig. 7 Structure of the HPEI TR-polymer.[116]

Supported CMS membranes are typically prepared by applying precursors on porous carriers for subsequent pyrolysis, and the choice of suitable porous materials is crucial. Nie *et al.*[119] developed CMS membranes supported on a novel porous carbon fiber (PCF) using wood tar as the precursor. These membranes exhibited moderate H_2/N_2 and H_2/CH_4 selectivity of 155 and 340, respectively, with an H_2 permeability of 86 barrer. In the pursuit of an economically viable coating and pyrolysis of porous materials, Cao *et al.*[120] fabricated multilayer asymmetric CMS membranes with outstanding gas separation properties. The membrane performance revealed an appealing CO_2/CH_4 selectivity of 58.8 and CO_2 permeability of 310 barrer at 35 °C. Additionally, Lee *et al.*[121] investigated the introduction of an alumina layer to prepare CMS membranes, highlighting the crucial role of the precursor solution viscosity in determining the membrane performance in gas separation. The CO_2 separation performances of different CMS membranes are summarized in Table 12.

It is evident that the CMS-600 membrane exhibited the highest permeability according to Table 12. This can be attributed to its fabrication process, involving the pyrolysis of a novel hydroxyl-containing polyetherimide (BAHPPF–6FDA-type HPEI) precursor. Upon heat treatment at 450 °C, the thermally reactive *ortho* OH groups in HPEI underwent a structural transformation, increasing the chain stiffness of the precursor membrane. Consequently, the derived CMS membrane possessed a more open pore structure, thereby enhancing its CO_2 permeability.[116]

The CMS membrane, known for its excellent chemical and thermal resistance, possessed a molecular size similar to polymer membranes and demonstrated exceptional selectivity in gas mixture separation with higher permeability. Despite these advantages, the current permeability of CMS membranes cannot satisfy commercial requirements. The pivotal challenge is enhancing the gas permeation, while preserving effective gas separation, a crucial aspect for advancing the development and application of CMS membranes.

3.3.5 PIM membranes. PIM membranes have emerged as highly appealing materials in the current landscape of membrane technology. In contrast to conventional polymers, PIM exhibits ultra-high permeability, establishing itself as the upper limit in nearly all gas separation performance metrics.[122]

By incorporating methanesulfonic acid (MSA), Han *et al.*[123] synthesized a PIM-1 membrane featuring carboxylic acid and

Table 12 Gas separation performances of some CMS membranes

Membrane	T (°C)	P (atm)	Permeability (barrer)	Selectivity
6F-DABA-75-CM576 membrane[115]	35	3.95	CO_2: 3573	CO_2/CH_4: 51.5
CMS-600 membrane[116]	30	1.08	CO_2: 15 060	CO_2/N_2: 26.8
PI100-600 membrane[117]	35	2	CO_2: 503	CO_2/CH_4: 56.5
Polysilsesquioxane CMS membrane[118]	35	1	CO_2: 354	CO_2/CH_4: 56
CMS70/PCF membrane[119]	35	2	CO_2: 14	CO_2/CH_4: 101
Multi-layer asymmetric CMS membrane[120]	35	1	CO_2: 310	CO_2/N_2: 58.8

triazinyl crosslinking (cPIM-1) (Fig. 8). The results indicated that the cPIM-1 membrane demonstrated the optimal overall CO_2 separation performance, with a permeability close to 11 511 barrer. The ideal selectivity for CO_2/N_2 and CO_2/CH_4 was 24.3 and 22.2, respectively. Additionally, PIM-1 mixed matrix membranes (MMMs) were created using polyhedral oligomeric silsesquioxane (POSS) and graphene oxide (GO) functionalized with POSS (GO–POSS) by Mohsenpour *et al.*[124] The MMM membrane containing 0.05 wt% GO–POSS exhibited a superior performance, with a CO_2 permeability of 12 000 barrer, representing a 69% increase compared to the pure PIM-1 membrane, while maintaining a similar selectivity (CO_2/CH_4 selectivity of 12 and CO_2/N_2 selectivity of 20.6).

Chen *et al.*[125] introduced a straightforward approach to concurrently enhance the permeability and CO_2 selectivity of PIM membranes by incorporating graphene oxide (GO) nanosheets, forming mixed matrix membranes. The GO nanosheets enhanced the hydrophilicity and surface roughness of the PIM-1 membrane, contributing to the porous nature of the mixed matrix membrane with a pore size of approximately 0.78 nm. This combination of properties significantly enhanced the gas separation performance of the PIM-1 membrane. The resulting membrane demonstrated an ultra-high CO_2 permeability of up to 6169 barrer and high CO_2/N_2 selectivity of 123.5, which is more than 7 times that of the pure PIM-1 membrane.

Similarly, Jeong *et al.*[126] developed an innovative CO_2 separation membrane by utilizing a polymer of intrinsic microporosity (PIM) and polyimide (PIM–PI) with high permeability as the hard segment and CO_2-philic PIM–polyethylene glycol/polypropylene glycol or PIM–PEG (poly(ethylene glycol))/PPG (poly(propylene glycol)) (as the soft segment) as a physical mixture. The resulting membrane exhibited high CO_2 permeability (1552.6 barrer) and CO_2/N_2 selectivity (29.3), approaching the upper bound defined by Robeson (2008) for gas separation performance.

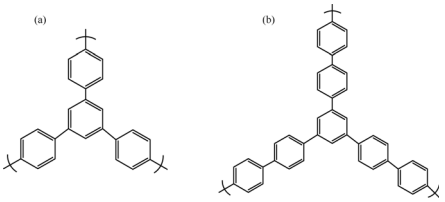

Fig. 8 Structure of (a) PPN1 and (b) PPN2.[123]

To enhance the gas separation performance of the PIM-1 membrane, extensive research has been conducted to manipulate its microporous structure. Recent advancements in PIM-based membranes were investigated by Shamsabadi *et al.*[127] Their study explored polymer synthesis strategies to modify the PIM structure, aiming to achieve an improved CO_2 separation performance and reduced physical aging. These strategies involved the utilization of monomers with suitable side chains, kinked segments, and stable structures.

In a separate effort to enhance the film durability, Sun *et al.*[128] hydrolyzed PIM-1 to produce a carboxyl PIM–COOH polymer. Subsequently, they employed propylene glycol to create mono-esterified PIM and conducted thermal ester crosslinking at various temperatures and durations. The resulting membrane treated at 300 °C for 8 h exhibited remarkable CO_2 permeability, CO_2/CH_4, and CO_2/N_2 selectivity values of 7421 barrer, 11.5, and 19.2, respectively, significantly surpassing the 2008 Robeson limit. The CO_2 separation performances of different PIM membranes are summarized in Table 13.

In Table 13, the GO–POSS72 membrane exhibited the highest permeability, which is attributed to the inclusion of porous nanoparticle (NP)-modified GO nanosheets within the membrane material. These nanoparticles created additional gas transport channels, enhancing the permeability. Moreover, the high aspect ratio of GO–POSS facilitated increased interactions with the polymer chains, aiding in suppressing physical aging phenomena and maintaining a high gas separation performance.[124]

In terms of enhancing the gas separation performance, the efficacy of CO_2 separation surpasses that of H_2. Notably, many hybrid membranes comprised of organic materials and PIM-1 demonstrated heightened CO_2 permeability and selectivity towards CO_2.[129] However, despite the efforts to mitigate physical aging through various strategies, it remains the primary challenge for industrial applications.

3.3.6 Facilitated transport membranes. The membrane material contains a reversible chemical reaction group of CO_2, which greatly enhances the dissolution of CO_2 molecules in the membrane, thereby effectively improved the permeability and selectivity for CO_2. This type of membrane is commonly referred to as a facilitated transport membrane. The inserted group,

Table 13 Gas separation performances of some PIM membranes

Membrane	T (°C)	P (atm)	Permeability (barrer)	Selectivity
cPIM-1/PPN2 membrane[123]	25	1.97	CO_2: 11 511	CO_2/N_2: 24.3
GO–POSS72 membrane[124]	25	0.99	CO_2: 12 000	CO_2/N_2: 20.6
PIM-1/GO mixed matrix membrane[125]	30	3.95	CO_2: 6169	CO_2/N_2: 123.5
PIM–PEG/PPG membrane[126]	30	1.97	CO_2: 1552.6	CO_2/N_2: 29.3
Mono-esterified PIM membrane[128]	35	1.97	CO_2: 7421	CO_2/N_2: 19.2

typically referred to as a carrier, distinguishes between a supported liquid membrane and a functional carrier membrane based on whether the carrier is an ion or a functional group. The functional carrier membrane, known for its superior stability and absence of carrier loss issues seen in supported liquid membranes, has attracted attention from researchers.

Currently, the amine group is the most widely utilized carrier. It is weakly alkaline and CO_2 is mildly acidic, and thus they can interact chemically in a way that is reversible. Liu[130] introduced a quaternary ammonium-based agglomerated zwitterionic material (pSBMA) in a CO_2 separation membrane, which significantly improved its CO_2 separation performance. According to the research, adding pSBMA increased the CO_2 permeability coefficient from 6.2 barrer to 49.8 barrer. Matsuyama *et al.*[131] prepared a CO_2 facilitated transport membrane by blending polyethyleneimine (PEI) and polyvinyl alcohol (PVA). At low pressure, the membrane had a CO_2/N_2 selectivity of 230.

Wang *et al.*[132] synthesized a macromolecule PETEDA (pentaerythrityl tetraethylenediamine) containing primary and secondary amine groups by the grafting method, and then blended it with PVA to prepare a CO_2-promoted transfer membrane. The performance tests showed that the optimal CO_2 permeability of the membrane was 81.4 barrer and the CO_2/CH_4 selectivity was 52. Taniguchi *et al.*[133] developed a crosslink agent, 4GMAP, by using a dendritic polymer and glycidyl methacrylate, and used 4GMAP to participate in the photopolymer reaction of polyethylene glycol dimethacrylate (PEGDMA) to prepare a carbon dioxide-promoting transfer membrane with a small membrane thickness. The membrane thickness was reduced from 640 μm to 9.5 μm. At a CO_2 partial pressure of 0.56 MPa at 313 K, the selectivity of the membrane for CO_2 reached 10 and its permeability to CO_2 was also greatly improved.

Winston *et al.*[134] synthesized a new type of facilitated transport membrane by coating a 170 nm selective layer on a polyether sulfone nanoporous substrate. In the selection layer, poly(*N*-vinyl formamide-vinylamine) covalently bonded to the polymer backbone was used as a fixed-site carrier, and an amino acid salt synthesized by deprotonating sarcosine with 2-(1-piperazinyl)ethylamine was mixed as a flow carrier. The membrane showed 975 barrer CO_2 permeability and over 140 CO_2/N_2 selectivity at 57 °C, 1 atm feed pressure and permeation pressure.

In addition to synthesizing new amine-containing carriers, researchers are also working on adjusting the structural orientation of polymers. Janakiram *et al.*[135] dispersed surface-modified nanocellulose in PVA to enhance the retention of water clusters in the polymer matrix. The thin composite film was synthesized by using sterically hindered polyamine as the fixed carrier and PZEA-Sar as the mobile carrier. At 35 °C, the thin film composite film had a CO_2 permeability of 652 barrer and CO_2/N_2 mixed gas selectivity of 41.

Researchers have also created various amine-free assisted transport membranes, in contrast to the usage of amine groups as carriers. Wang *et al.*[136] found that carboxyl groups can also be used as CO_2 transfer carriers through experiments. A CO_2 facilitated transfer membrane was prepared with P(AAS-*co*-AAM) as the separation layer and PSF as the support layer. When the operating pressure was 1 bar, the membrane had a CO_2 permeability of 98 barrer and CO_2/N_2 mixed gas selectivity of 70.

Yao *et al.*[137] prepared a membrane for promoting transfer that is similar to carbonic anhydrase (CA), which is used by organisms to effectively catalyze the conversion of CO_2 into water. The results showed that the CO_2 permeability exceeded 1000 barrer and the CO_2/N_2 selectivity was 83, showing good gas permeability and selectivity. The CO_2 separation performances of different facilitated transport membranes are summarized in Table 14.

Based on the data presented in Table 14, the poly(amidoamine) dendritic-containing polymer membrane exhibited the highest permeability and selectivity. This membrane was prepared by physically immobilizing polyamide amide (PAMAM) dendrimers within cross-linked polyethylene glycol (PEG) through the photopolymerization of PEG dimethacrylate (PEGDMA) in the presence of dendrimers in ethanol. The immiscibility between the PEG matrix and dendritic macromolecules resulted in the formation of a bicontinuous phase separation structure on the micrometer scale. This structure inhibited a reduction in the membrane thickness, thereby enhancing the CO_2 permeability and selectivity.[133]

When comparing transfer membranes with traditional organic membranes for carbon dioxide separation, it is essential to note that the former not only relies on the carrier for facilitating the transfer process but also involves a dissolution–penetration–diffusion process similar to that of traditional organic membranes. Transfer membranes theoretically exhibit a higher gas separation efficiency than traditional organic membranes.

Table 14 Gas separation performances of some facilitated transport membranes

Membrane	T (°C)	P (atm)	Permeability (barrer)	Selectivity
pSBMA membrane[130]	35	1.97	CO_2: 104	CO_2/CH_4: 82
Macromolecule PETEDA membrane[132]	27	1.89	CO_2: 81.4	CO_2/CH_4: 82
Poly(amidoamine) dendrimer-containing polymeric membrane[134]	57	1	CO_2: 975	CO_2/N_2: 140
Thin composite membrane[135]	35	1.68	CO_2: 652	CO_2/N_2: 41
CO_2-facilitated transfer membrane[136]	30	4.93	CO_2: 98	CO_2/N_2: 70
Poly(*N*-vinylimidazole)–zinc membrane[137]	30	0.99	CO_2: 1000	CO_2/N_2: 83

However, the permeability and selectivity values mentioned appeared to be comparable to that of previously described membranes. This is primarily because the water content and pressure of the feed gas significantly influence the carbon dioxide transfer through the membrane, consequently impacting its performance. Therefore, the permeability and selectivity of transfer membranes may not demonstrate significant advantages in certain scenarios.

In the case of gas permeability, facilitated transport membranes theoretically have a better separation performance than conventional organic membranes. Between them, functional carrier membranes had the advantages of good stability and simple operation. However, a clear description and mechanism of the CO_2 promoting transfer process within functional carrier membranes is lacking. If the mechanism of the CO_2 promoting transfer in these membranes can be clarified, it would be beneficial to address any shortcomings and further enhance their gas separation and permeation performance. This aspect is expected to become the focus in research and development of gas separation membranes in the future.

3.4 Application scenario of membranes

Membranes with different structures have different gas separation characteristics and Fig. 9–11 and Table S2, ESI† outline the gas separation performances and typical application scenarios of diverse membranes, including CO_2/N_2 separation, CO_2/H_2 separation, and CO_2/CH_4 separation. These application scenarios correspond to post-combustion CO_2 capture, pre-combustion CO_2 capture, and natural gas desulfurization, respectively.

It can be seen in Fig. 9–11 that for inorganic membranes, silica membranes are mainly used to investigate the application of CO_2/H_2 and CO_2/CH_4 separation, zeolite membranes tend to be used in CO_2/N_2 and CO_2/CH_4 separation, and graphene membranes focus more on CO_2/N_2 separation. Cellulose membranes, polyamide membranes, and polysulfone membranes tend to be used for CO_2/N_2 and CO_2/CH_4 separation, while polyether membranes are also partially used for CO_2/H_2 separation.

Among the emerging membranes, composite membranes and MOF membranes are more used for CO_2/N_2 and CO_2/CH_4 separation. ZIF membranes are mainly biased towards CO_2/H_2 separation. CMS is mainly used for CO_2/CH_4 separation, and some used for CO_2/N_2 separation. PIM is mostly used for CO_2/CH_4 separation, while facilitated transport membranes are mainly used for CO_2/N_2 separation, and a small part used for CO_2/CH_4 separation.

4. Challenges and perspectives

The membrane materials serve as the foundation of membrane separation technology, given that their performance directly impacts the potential applications of this technology. Fig. S1 in the ESI† outlines the gas separation performances of diverse membranes and the gas separation membranes with a Robeson

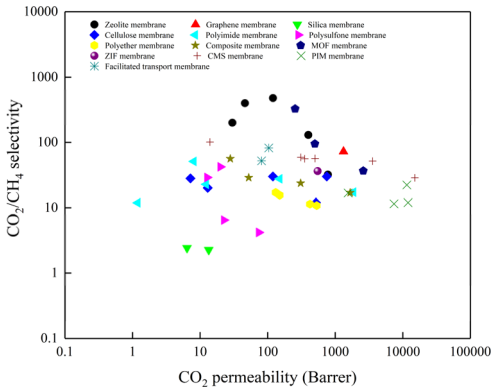

Fig. 9 CO_2/CH_4 gas separation performance of different types of membranes.

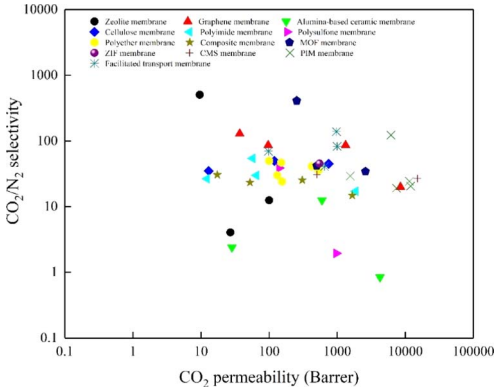

Fig. 10 CO_2/N_2 gas separation performance of different types of membranes.

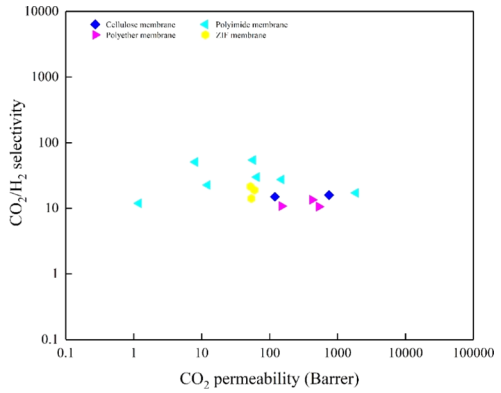

Fig. 11 CO_2/H_2 gas separation performance of different types of membranes.

upper limit for permeability and selectivity, indicating that higher permeability resulted in lower selectivity, and *vice versa*. Therefore, in practical applications, membrane materials are selected based on the separation requirements, operating conditions and other relevant factors. Gas separation membranes can be classified into three groups including inorganic membranes, organic membranes, and emerging membranes.

Currently, the commonly used organic and inorganic membranes have unique merits and drawbacks. Advanced materials such as composite membranes, MOF membranes, ZIF membranes, CMS membranes, PIM membranes, and facilitated transport membranes have been developed to overcome existing challenges and present new opportunities. The introduction of novel materials has the potential to address multiple issues simultaneously but also poses new challenges. Thus, further research is essential to advance the development of CO_2 separation membranes with high permeability and selectivity, as follows:

(1) An optimal inorganic membrane should exhibit consistent permeability and selectivity for CO_2, while overcoming processing challenges.

(2) The development of new organic membranes should prioritize enhanced resistance to high temperatures and pressures, superior thermal stability, and mechanical strength. Simultaneously, the membranes should be easy to process, improving their anti-plasticization capabilities.

(3) Due to the presence of organic and inorganic phases in composite membranes, defects at the phase interface lead to poor compatibility between the two phases and the poor dispersion of inorganic nanoparticles on organic membranes is also a problem to be solved.

(4) Further investigations are required to delve into the adsorption, diffusion, and distribution mechanisms of gases in MOF membranes. In the case of ZIF membranes, the primary focus should be on enhancing their separation selectivity for H_2 and CO_2, while concurrently addressing challenges related to their mechanical strength, particularly in high-pressure applications. The paramount challenge for CMS membranes is augmenting the gas permeation without compromising effective gas separation. Lastly, the industrial application of PIM membranes is primarily hindered by physical aging, signifying a crucial hurdle that warrants attention.

(5) The supported liquid membrane in facilitated transport membranes exhibits poor stability, necessitating consideration for carrier loss mitigation to enhance its stability. Additionally, carrier saturation should be considered in functional carrier membranes to ensure their optimal performance.

5. Conclusions

The issue of global warming, stemming from the escalating carbon dioxide levels, poses a severe environmental challenge. Accordingly, it is urgent to develop carbon dioxide treatment technology that is not only environmentally friendly but also highly efficient with low energy consumption. In this case, membrane separation technology, characterized by its simplicity and high effectiveness, has attracted increasing attention from researchers. Membrane separation technology is based on the acquisition of membranes with high permeability and selectivity. Herein, we provided an overview of various CO_2 separation membranes, including inorganic membranes, organic membranes, and emerging membranes. Additionally, we introduced the characteristics and progress of typical membranes. The primary findings were summarized as follows.

Inorganic membranes exhibit a narrow and controllable pore size distribution, excellent gas selectivity and permeability, as well as high temperature and pressure resistance. However, the fabrication of inorganic membranes is challenging, limiting their application in the field of gas separation. Organic membranes, fabricated from materials such as cellulose, polyamide, polysulfone, and polyether demonstrate effective CO_2 separation capabilities. Nevertheless, many organic membranes are associated with challenges such as poor anti-pollution and poor mechanical properties, thereby limiting their broader application in CO_2 gas separation.

Emerging CO_2 membranes, such as composite membranes and MOF membranes, exhibit superior CO_2 separation performances compared to conventional membrane materials. However, the primary challenge is maintaining effective gas separation, while enhancing gas permeability for their industrial application. Additionally, there is still a long way to go to transform their theoretical high gas permeability and selectivity into reality.

In conclusion, a multitude of advanced membranes have been investigated, significantly promoting the progress of membrane technology. To actualize the ultimate application of CO_2 membrane separation in the future, a collaborative advancement in membrane technology, chemical science, and engineering applications should be developed.

Conflicts of interest

There are no conflicts to declare.

Acknowledgements

The work was supported by the National Natural Science Foundation of China (52274029).

Notes and references

1 S. Yuan, D. Ma, J. Li, T. Zhou, Z. Ji and H. Han, *Petrol. Explor. Dev.*, 2022, **49**, 828–834.
2 Z. Zhao, S. Yao, S. Yang and X. Wang, *Environ. Sci.*, 2022, **44**, 1128–1138.
3 S. Feng, J. Ren, X. Ren, H. Li, K. Hua and M. Deng, *Membr. Sci. Technol.*, 2012, **32**, 27–33.
4 X. Bu, *Clean Coal Technol.*, 2014, **20**, 9–13.
5 H. B. Park, J. Kamcev, L. M. Robeson, M. Elimelech and B. D. Freeman, *Science*, 2017, **356**, eaab0530.
6 M. Robeson, *J. Membr. Sci.*, 2010, **320**, 390–400.
7 L. Zhu, Masteral thesis, Dalian University of Technology, 2010.
8 D. Yang and M. Xu, *Inn. Mong. Petrochem. Ind.*, 2004, **30**, 28–31.
9 X. Ruan, X. Yan, Y. Dai and G. He, *Petrochem. Technol.*, 2015, **44**, 785–790.
10 Y. Zhao and W. S. W. Ho, *Ind. Eng. Chem. Res.*, 2012, **52**, 8774–8782.
11 R. J. R. Uhlhorn, M. H. B. J. Huisin'tveld, K. Keizer and A. J. Burggraaf, *J. Mater. Sci. Lett.*, 1989, **8**, 1135–1138.
12 R. Igi, T. Yoshioka, Y. H. Ikuhara and Y. Iwamoto, *J. Am. Ceram. Soc.*, 2008, **91**, 2975–2981.
13 J. Yan, Q. Wei, X. Duan, J. He, Q. Li and Z. Nie, *Chin. J. Inorg. Chem.*, 2011, **27**, 1334–1340.
14 W. Li, D. Li, L. Zheng, J. Fan and Z. Zhang, *J. Chin. Ceram. Soc.*, 2014, **42**, 416–422.
15 Y. Gu, P. Hacarlioglu and S. T. Oyama, *J. Membr. Sci.*, 2008, **310**, 28–37.
16 Z. Zhang, L. Zheng, D. Li and W. Li, *J. Shenyang Univ. Chem. Technol.*, 2014, **28**, 308–313.
17 Z. Hong, Q. Wei, G. Li, X. Wang, Z. Nie and Q. Li, *Chin. J. Inorg. Chem.*, 2013, **29**, 941–947.
18 Y. Ding, Q. Wei, X. Liu, Q. Li and Z. Nie, *Membr. Sci. Technol.*, 2014, **34**, 22–27.
19 D. Uhlmann, S. Liu, B. P. Ladewig and J. C. D. da Costa, *J. Membr. Sci.*, 2009, **326**, 316–321.
20 N. Xu, *Chem. Ind. Eng. Prog.*, 2000, **4**, 5–9.
21 J. Wang, J. Yang, Z. Chen and D. Yin, *Membr. Sci. Technol.*, 2011, **31**, 118–126.
22 E. E. Mcleary, J. C. Jansen and F. Kapteijn, *Microporous Mesoporous Mater.*, 2006, **90**, 198–220.
23 J. Wang, J. Yang, H. Li and L. Li, *Membr. Sci. Technol.*, 2014, **34**, 1–7.
24 S. Himeno, T. Tomita, K. Suzuki, K. Nakayama and K. Yajima, *Ind. Eng. Chem. Res.*, 2007, **46**, 6989–6997.
25 Y. Cui, H. Kita and K.-i. Okamoto, *Chem. Commun.*, 2003, **17**, 2154–2155.
26 H. Gong, Masteral thesis, Northeastern University, 2018.
27 E. Jang, S. Hong, E. Kim, N. Choi, S. J. Cho and J. Choi, *J. Membr. Sci.*, 2018, **549**, 46–59.
28 K. Kida, Y. Maeta and K. Yogo, *Sep. Purif. Technol.*, 2018, **197**, 116–121.
29 J. Zhou, F. Gao, K. Sun, X. Jin, Y. Zhang, B. Liu and R. Zhou, *Energy Fuels*, 2020, **34**, 11307–11314.
30 L. Yu, A. Holmgren, M. Zhou and J. Hedlund, *J. Mater. Chem. A*, 2018, **6**, 6847–6853.
31 J. C. White, P. K. Dutta, K. Shqau and H. Verweij, *Langmuir*, 2010, **26**, 10287–10293.
32 L. Li and J. Yang, *Membr. Sci. Technol.*, 2022, **42**, 138–145.
33 Z. Cao, N. Anjikar and S. Yang, *Separations*, 2022, **9**, 9020047.
34 L. Yang, W. Luo, C. Wang and C. Xu, *J. Inorg. Mater.*, 2020, **35**, 959–971.
35 D.-e. Jiang, V. R. Cooper and D. Sheng, *Nano Lett.*, 2009, **9**, 4019–4024.
36 S. Wang, S. Dai and D. E. Jiang, *ACS Appl. Nano Mater.*, 2018, **2**, 379–384.
37 K. Celebi, J. Buchheim, R. M. Wyss, A. Droudian, P. Gasser, I. Shorubalko, J.-I. Kye, C. Lee and H. G. Park, *Science*, 2014, **344**, 289–292.
38 C. Ma, M. Wang, Z. Wang, M. Gao and J. Wang, *J. CO2 Util.*, 2020, **42**, 101296.
39 H. W. Kim, H. W. Yoon, S.-M. Yoon, B. M. Yoo, B. K. Ahn and Y. H. Cho, *Science*, 2013, **342**, 91–95.
40 H. Li, Z. Song, X. Zhang, Y. Huang, S. Li and Y. Mao, *Science*, 2013, **342**, 95–98.
41 C. Chi, X. Wang, Y. Peng, Y. Qian and Z. Hu, *Chem. Mater.*, 2016, **28**, 2921–2927.
42 Y. Zhang, S. Zhang and T. S. Chung, *Environ. Sci. Technol.*, 2015, **49**, 10235–10242.
43 J. W. Burress, S. Gadipelli and J. Ford, *Angew. Chem.*, 2010, **49**, 8902–8904.
44 M. Karunakaran, L. F. Villalobos, M. Kumar, R. Shevate, F. H. Akhtar and K.-V. Peinemann, *J. Mater. Chem. A*, 2017, **5**, 649–656.
45 Q. Xin, F. Ma, L. Zhang, S. Wang, Y. Li, H. Ye, X. Ding, L. Lin, Y. Zhang and X. Cao, *J. Membr. Sci.*, 2019, **586**, 23–33.
46 J. Shen, M. Zhang, G. Liu and W. Jin, *RSC Adv.*, 2016, **6**, 54281–54285.
47 J. Shen, G. Liu, K. Huang, Z. Chu, W. Jin and N. Xu, *ACS Nano*, 2016, **10**, 3398–3409.
48 B. Shimekit, H. Mukhtar, F. Ahmad and S. Maitra, *Trans. Indian Ceram. Soc.*, 2009, **68**, 115–138.
49 Y.-K. Cho, K. Han and K.-H. Lee, *J. Mater. Sci.*, 1995, **104**, 219–230.
50 B. Kang and H. Sang, *J. Mater. Sci.*, 1999, **34**, 1391–1398.
51 T. Isobe, Y. Takada, S. Matsushita and A. Nakajima, *Ceram. Int.*, 2015, **41**, 7759–7765.
52 K. Shankar and P. Kandasamy, *Greenhouse Gases: Sci. Technol.*, 2019, **9**, 287–305.
53 S. K. Sharma, B. K. Sanfui, A. Katare and B. Mandal, *ACS Appl. Mater. Interfaces*, 2020, **12**, 40269–40284.
54 J. Yang, J. Li, N. Cui, N. Cheng and M. Guo, *Coal Chem. Ind.*, 2019, **42**, 119–125.
55 C. Gao, L. Cai, F. Dong, H. Xie, S. Qin and Q. Zheng, *J. Chem. Eng. Chin. Univ.*, 2019, **33**, 1037–1047.

56 J. Hao, Z. Wang and S. Wang, *Polym. Mater. Sci. Eng.*, 1997, **13**, 65–69.
57 J. Wu, PhD thesis, Dalian Institute of Chemical Physics, Chinese Academy of Sciences, 2002.
58 X. Jie, PhD thesis, Dalian Institute of Chemical Physics, Chinese Academy of Sciences, 2005.
59 L. Ansaloni, J. Salas-Gay, S. Ligi and M. G. Baschetti, *J. Membr. Sci.*, 2017, **522**, 216–225.
60 H. T. Lu, S. Kanehashi, C. A. Scholes and S. E. Kentish, *J. Membr. Sci.*, 2017, **539**, 432–440.
61 X. Shang, S. Chen, X. Shi and Z. Zhu, *Chin. J. Chem. Phys.*, 1997, **10**, 92–97.
62 C. Zhang, Y. Weng and W. Han, *Sci. Sin.: Chim.*, 2020, **50**, 655–668.
63 Y. Zhuang, J. G. Seong, Y. S. Do, H. J. Jo, M. J. Lee, G. Wang, M. D. Guiver and Y. M. Lee, *Macromolecules*, 2014, **47**, 7947–7957.
64 P. Sysel, D. Maly, J. Vysohlid, K. Friess, K. Pilnacek, M. Lanc and O. Vopicka, *Polym. Eng. Sci.*, 2017, **57**, 1367–1373.
65 F. Jianhua, K. Hidetoshi and O. Ken-ichi, *J. Membr. Sci.*, 2001, **182**, 245–256.
66 E. M. Maya, D. M. Muñoz, J. G. Campa, J. D. Abajo and Á. E. Lozano, *Desalination*, 2006, **199**, 188–190.
67 C. Zhang, L. Pei and C. Bing, *J. Membr. Sci.*, 2017, **528**, 206–216.
68 T. Zhu, Masteral thesis, Taiyuan University of Technology, 2018.
69 H. Si, H. Jia, P. Jiang, S. Zhao and S. Zhang, *Journal of Qiqihar University (Natural Science Edition)*, 2021, **37**, 77–80.
70 H. Eguchi, D. J. Kim and W. J. Koros, *Polymer*, 2015, **58**, 121–129.
71 M. Zhang, Masteral thesis, Taiyuan University of Technology, 2015.
72 X. He, Masteral thesis, Taiyuan University of Technology, 2018.
73 S. Shahid and K. Nijmeijer, *Sep. Purif. Technol.*, 2017, S1383586617307852.
74 H. A. Mannan, H. Mukhtar, M. S. Shaharun, M. R. Othman and T. Murugesan, *J. Appl. Polym. Sci.*, 2016, **133**, 42496.
75 Y. Meng, Masteral thesis, Lanzhou University of Technology, 2020.
76 L. Meng, Masteral thesis, Tiangong University, 2016.
77 X. Zhou, J. Yan, H. Gao, A. Wang and Y. Bai, *N. Chem. Mater.*, 2018, **46**, 195–199.
78 Y. Wang, J. Ren, C. Xu, H. Li, S. Feng and M. Deng, *Membr. Sci. Technol.*, 2014, **34**, 27–32.
79 Q. Zhao, S. He, J. Lin and Q. Lin, *China Plast.*, 2019, **33**, 13–20.
80 A. Car, C. Stropnik, W. Yave and K.-V. Peinemann, *J. Membr. Sci.*, 2008, **307**, 88–95.
81 S. R. Reijerkerk, M. H. Knoef, K. Nijmeijer and M. Wessling, *J. Membr. Sci.*, 2010, **352**, 126–135.
82 X. Xiao, X. Xu, X. Li, J. Dong, X. Zhao and Q. Zhang, *Acta Polym. Sin.*, 2022, **53**, 505–513.
83 Z. Wang, X. Liu, X. Li, Z. Tao, P. Yu, Q. Zhang and H. Shi, *Shandong Chem. Ind.*, 2021, **50**, 74–75+79.
84 Y. Cao, C. Yang and W. Wang, *Spec. Petrochem.*, 2015, **32**, 53–60.
85 W. Wang, X. Jiang, Y. Li, L. Su, Y. Zou and Z. Tong, *CIESC J.*, 2020, **71**, 3807–3818.
86 Y. Cheng, Y. Ying, S. Japip, S.-D. Jiang and T.-S. Chung, *Adv. Mater.*, 2018, **30**, e1802401.
87 X. Gong, L. Zhu, Y. Xu and B. Zhu, *Membr. Sci. Technol.*, 2011, **31**, 89–93.
88 L. Y. Jiang, T. S. Chung and S. Kulprathipanja, *AIChE J.*, 2010, **52**, 2898–2908.
89 T. Wu, Y. Shi, Y. Liu, I. Kumakiri, K. Tanaka, X. Chen and H. Kita, *Energy Fuels*, 2021, **35**, 10680–10688.
90 M. Mubashir, Y. Y. Fong, L. K. Keong, C. T. Leng and N. Jusoh, *Sep. Purif. Technol.*, 2018, **199**, 140–151.
91 B. Liu, PhD thesis, Harbin Institute of Technology, 2021.
92 C. Li, Masteral thesis, China University of Petroleum, Beijing, 2019.
93 Y. Gao, Masteral thesis, Shenyang University of Technology, 2021.
94 E. Adatoz, A. K. Avci and S. Keskin, *Sep. Purif. Technol.*, 2015, **152**, 207–237.
95 Q. Qian, P. A. Asinger, M. J. Lee, G. Han, K. M. Rodriguez, S. Lin, F. M. Benedetti, A. X. Wu, W. S. Chi and Z. P. Smith, *Chem. Rev.*, 2020, **120**, 8161–8266.
96 Z. Rui, J. B. James, A. Kasik and Y. S. Lin, *AIChE J.*, 2016, **62**, 3836–3841.
97 D. S. Chiou, H. J. Yu, T. H. Hung, Q. Lyu, C. K. Chang, J. S. Lee, L. C. Lin and D. Y. Kang, *Adv. Funct. Mater.*, 2020, **31**, 2006924.
98 E. V. Perez, K. J. Balkus, J. P. Ferraris and I. H. Musselman, *J. Membr. Sci.*, 2009, **328**, 165–173.
99 Y. Wang, H. Jin, Q. Ma, K. Mo, H. Mao, A. Feldhoff, X. Cao, Y. Li, F. Pan and Z. Jiang, *Angew. Chem., Int. Ed.*, 2020, **59**, 4365–4369.
100 J. Fu, S. Das, G. Xing, T. Ben, V. Valtchev and S. Qiu, *J. Am. Chem. Soc.*, 2016, **138**, 7673–7680.
101 M. Bu, Y. Feng, Q. Li, Y. Wang, S. Feng, K. Zhang, Y. Jiang, L. Fan, Z. Kang and D. Sun, *Inorg. Chem. Front.*, 2021, **8**, 5016–5023.
102 R. Hardian, J. Jia, A. Diaz-Marquez, S. Naskar, D. Fan, O. Shekhah, G. Maurin, M. Eddaoudi and G. Szekely, *Adv. Mater.*, 2024, **36**, 2314206.
103 D.-Y. Kang and J. S. Lee, *Langmuir*, 2023, **39**, 2871–2880.
104 Y. Li, F. Liang, H. Bux, W. Yang and J. Caro, *J. Membr. Sci.*, 2010, **354**, 48–54.
105 H. Chang, Y. Wang, L. Xiang, D. Liu, C. Wang and Y. Pan, *Chem. Eng. Sci.*, 2018, **192**, 85–93.
106 J. Liu, C. Liu and A. Huang, *Int. J. Hydrogen Energy*, 2020, **45**, 703–711.
107 P.-H. Chang, Y.-T. Lee and C.-H. Peng, *Materials*, 2020, **13**, 5009.
108 J.-W. Wang, N.-X. Li, Z.-R. Li, J.-R. Wang, X. Xu and C.-S. Chen, *Ceram. Int.*, 2016, **42**, 8949–8954.
109 M. Jia, X.-F. Zhang, Y. Feng, Y. Zhou and J. Yao, *J. Membr. Sci.*, 2020, **595**, 117579.

110 T.-M. T. Nguyen, J.-W. Chen, M.-T. Pham, H. M. Bui, C.-C. Hu, S.-J. You and Y.-F. Wang, *Environ. Technol. Innov.*, 2023, **31**, 103169.
111 Y. Song, M. He, J. Zhao and W. Jin, *Sep. Purif. Technol.*, 2021, **270**, 118722.
112 L. Lang, F. Banihashemi, J. B. James, J. Miao and J. Y. S. Lin, *J. Membr. Sci.*, 2021, **619**, 118743.
113 Z. Lai, *Curr. Opin. Chem. Eng.*, 2018, **20**, 78–85.
114 L. Li, R. Xu, C. Song, B. Zhang, Q. Liu and T. Wang, *Membranes*, 2018, **8**, 134.
115 Q. Wang, F. Huang, C. J. Cornelius and Y. Fan, *J. Membr. Sci.*, 2021, **621**, 118785.
116 M. Hou, L. Li, Z. He, R. Xu, Y. Lu, J. Zhang, Z. Pan, C. Song and T. Wang, *J. Membr. Sci.*, 2022, **656**, 120639.
117 J. M. Pérez-Francisco, J. L. Santiago-García, M. I. Loría-Bastarrachea, D. R. Paul, B. D. Freeman and M. Aguilar-Vega, *J. Membr. Sci.*, 2020, **597**, 117703.
118 J. H. Shin, H. J. Yu, H. An, A. S. Lee, S. S. Hwang, S. Y. Lee and J. S. Lee, *J. Membr. Sci.*, 2019, **570–571**, 504–512.
119 J. Nie, F. Okada, H. Kita, K. Tanaka, T. Mihara, D. Kondo, Y. Yamashita and N. Yahagi, *Energy Fuels*, 2022, **36**, 7147–7157.
120 Y. Cao, K. Zhang, O. Sanyal and W. J. Koros, *Angew. Chem., Int. Ed.*, 2019, **58**, 12149–12153.
121 P.-S. Lee, D. Kim, S.-E. Nam and R. R. Bhave, *Microporous Mesoporous Mater.*, 2016, **224**, 332–338.
122 Y. Wang, B. S. Ghanem, Z. Ali, K. Hazazi, Y. Han and I. Pinnau, *Small Struct.*, 2021, **2**, 210049.
123 W. Han, C. Zhang, M. Zhao, F. Yang, Y. Yang and Y. Weng, *J. Membr. Sci.*, 2021, **636**, 119544.
124 S. Mohsenpour, A. W. Ameen, S. Leaper, C. Skuse, F. Almansour, P. M. Budd and P. Gorgojo, *Sep. Purif. Technol.*, 2022, **298**, 121447.
125 M. Chen, F. Soyekwo, Q. Zhang, C. Hu, A. Zhu and Q. Liu, *J. Ind. Eng. Chem.*, 2018, **63**, 296–302.
126 I. Jeong, I. Hossain, A. Husna and T. H. Kim, *Macromol. Mater. Eng.*, 2022, **308**, 2200596.
127 A. A. Shamsabadi, M. Rezakazemi, F. Seidi, H. Riazi, T. Aminabhavi and M. Soroush, *Prog. Energy Combust. Sci.*, 2021, **84**, 100903.
128 Y. Sun, J. Zhang, H. Li, F. Fan, Q. Zhao, G. He and C. Ma, *Sep. Purif. Technol.*, 2023, **314**, 123623.
129 S. He, B. Zhu, S. Li, Y. Zhang, X. Jiang, C. H. Lau and L. Shao, *Sep. Purif. Technol.*, 2022, **284**, 120277.
130 Y. Liu, Masteral thesis, Tianjin University, 2015.
131 M. Hideto, T. Akihiro, N. Tadashi and K. Yoshiiro, *J. Membr. Sci.*, 1999, **163**, 221–227.
132 Z. Wang, M. Li, Y. Cai, J. Wang and S. Wang, *J. Membr. Sci.*, 2007, **290**, 250–258.
133 I. Taniguchi, T. Kai, S. Duan, S. Kazama and H. Jinnai, *J. Membr. Sci.*, 2015, **475**, 175–183.
134 Z. Tong and W. S. W. Ho, *Sep. Sci. Technol.*, 2016, **52**, 156–167.
135 S. Janakiram, X. Yu, L. Ansaloni, Z. Dai and L. Deng, *ACS Appl. Mater. Interfaces*, 2019, **11**, 33302–33313.
136 M. Wang, Z. Wang, J. Wang, Y. Zhu and S. Wang, *Energy Environ. Sci.*, 2011, **4**, 3955–3959.
137 Y. Kai, W. Zhi, W. Jixiao and W. Shichang, *Chem. Commun.*, 2012, **48**, 1766–1768.